Appendix A
Mie Coefficients

As discussed in Sect. 3.3.3, the Mie coefficients a_n and b_n are precisely given by Bessel functions.[1] On the other hand, Deirmendjian (1969) showed that they were also derivable by means of the recursion formula. The derivation has been reviewed in varied ways by predecessors (e.g., Ulaby et al. 1981, pp. 290–291, 1986, pp. 2129–2132). Present appendix will be another collection which briefly presents the derivation by recursion formula after Deirmendjian (1969, Chap. 2).

These coefficients can be expressed by the Riccati–Bessel functions,[2] $\psi_n(x)$ and $\zeta_n(x)$, as (Van de Hulst 1957, p. 123)

[1] Bessel functions are defined as the canonical solutions $y(x)$ of Bessel's differential equation;

$$x^2\frac{\mathrm{d}^2y}{\mathrm{d}x^2}+x\frac{\mathrm{d}y}{\mathrm{d}x}+(x^2-\alpha^2)y=0.$$

If α is integer n, the solutions are given by Bessel function of the first kind $J_n(x)$ and that of the second kind $Y_n(x)$. Moreover, for the spherical Bessel differential equation

$$x^2\frac{\mathrm{d}^2y}{\mathrm{d}x^2}+2x\frac{\mathrm{d}y}{\mathrm{d}x}+x^2-n(n+1)y=0,$$

two linear independent solutions are expressed by the spherical Bessel functions $j_n(x)$ and $y_n(x)$, which are in the following relationships with $J_n(x)$ and $Y_n(x)$, respectively;

$$j_n(x)=\sqrt{\frac{\pi}{2x}}J_{n+1/2}(x),\quad y_n(x)=\sqrt{\frac{\pi}{2x}}Y_{n+1/2}(x)=(-1)^{n+1}\sqrt{\frac{\pi}{2x}}(-1)^{n+1}J_{-n-1/2}(x).$$

[2] Riccati–Bessel functions are expressed using Bessel function and the spherical Bessel functions as

$$\psi_n(x)=xj_n(x)=\sqrt{\frac{\pi x}{2}}J_{n+1/2}(x),\quad \xi_n(x)=-xy_n(x)=\sqrt{\frac{\pi x}{2}}Y_{n+1/2}(x),\quad \zeta_n(x)=\psi_n(x)+j\xi_n(x).$$

S. Fukao and K. Hamazu, *Radar for Meteorological and Atmospheric Observations*,
DOI 10.1007/978-4-431-54334-3, © Springer Japan 2014

$$a_n = \frac{A_n(y)\psi_n(x) - m\psi_n'(x)}{A_n(y)\zeta_n(x) - m\zeta_n'(x)}, \tag{A.1}$$

$$b_n = \frac{mA_n(y)\psi_n(x) - \psi_n'(x)}{mA_n(y)\zeta_n(x) - m\zeta_n'(x)}, \tag{A.2}$$

where $'$ denotes derivative. Functions $\psi_n(x)$ and $\zeta_n(x)$ can be expressed using $(n+1/2)$th Bessel function of the first kind[3] $J_{n+1/2}$, and that of the second kind $Y_{n+1/2}$ as

$$\psi_n(x) = x j_n(x) = \sqrt{\frac{\pi x}{2}} J_{n+1/2}(x), \tag{A.3}$$

$$\begin{aligned}\zeta_n(x) &= \sqrt{\frac{\pi x}{2}} J_{n+1/2}(x) - jY_{n+1/2}(x) \\ &= \sqrt{\frac{\pi x}{2}} [J_{n+1/2}(x) + (-1)^n jJ_{-n-1/2}(x)].\end{aligned} \tag{A.4}$$

In (A.1) and (A.2), $A_n(y)$ is adopted to separate the functions with argument y from those with argument x, and defined as

$$A_n(y) \equiv \frac{\psi_n'(y)}{\psi_n(y)}, \quad y \equiv mx = m\frac{\pi D}{\lambda}, \tag{A.5}$$

where m is the complex refractive index, D the diameter of the sphere, and λ the wavelength in free space. For absorbing spheres such as raindrops, m is complex. Thus, $A_n(y)$ depends on Bessel functions of complex argument.

Using the characteristics of Bessel function of the first kind for half integer, derivatives of (A.3) and (A.4) become as follows;

$$\psi_n'(x) = \frac{\mathrm{d}}{\mathrm{d}x}\left[\sqrt{\frac{\pi x}{2}} J_{n+1/2}(x)\right] = \sqrt{\frac{\pi x}{2}}\left[J_{n-1/2}(x) - \frac{n}{x} J_{n+1/2}(x)\right], \tag{A.6}$$

[3] Bessel function of the first kind $J_{n+1/2}(x)$ for half integer $n+1/2$ can be expressed as

$$J_{1/2}(x) = \sqrt{\frac{2}{\pi x}}\sin x, \quad J_{-1/2}(x) = \sqrt{\frac{2}{\pi x}}\cos x,$$

$$J_{3/2}(x) = \frac{1}{x}J_{1/2}(x) - J_{-1/2}(x) = \sqrt{\frac{2}{\pi x}}\left(\frac{\sin x}{x} - \cos x\right),$$

$$J_{-3/2}(x) = -\frac{1}{x}J_{-1/2}(x) - J_{1/2}(x) = \sqrt{\frac{2}{\pi x}}\left(\frac{\cos x}{x} + \sin x\right),$$

$$J_{n+1/2}(x) = \frac{2(n-\frac{1}{2})}{x}J_{n-1/2}(x) - J_{n-3/2}(x), \quad J_{n+1/2}'(x) = \frac{1}{2}J_{n-1/2}(x) - \frac{1}{2}J_{n+3/2}(x),$$

$$\frac{\mathrm{d}}{\mathrm{d}x}\left[\sqrt{\frac{\pi x}{2}}J_{-n-1/2}(x)\right] = -\sqrt{\frac{\pi x}{2}}\left[J_{-n+1/2}(x) + \frac{n}{x}J_{-n-1/2}(x)\right], \tag{A.7}$$

$$\zeta_n'(x) = \sqrt{\frac{\pi x}{2}}\left\{J_{n-1/2}(x) - \frac{n}{x}J_{n+1/2}(x) - (-1)^n j\left[J_{-n+1/2}(x) + \frac{n}{x}J_{-n-1/2}(x)\right]\right\}. \tag{A.8}$$

Substituting (A.3)–(A.8) into (A.1) and (A.2), the Mie coefficients become

$$\begin{aligned} a_n(m,\, x) = &\left\{\left[\frac{A_n(y)}{m} + \frac{n}{x}\right]J_{n+1/2}(x) - J_{n-1/2}(x)\right\} \\ &\times\left\{\left[\frac{A_n(y)}{m} + \frac{n}{x}\right]\left[J_{n+1/2}(x) + (-1)^n jJ_{-n-1/2}(x)\right]\right. \\ &\left. - \left[J_{n-1/2}(x) - (-1)^n jJ_{-n+1/2}(x)\right]\right\}^{-1} \end{aligned} \tag{A.9}$$

and

$$\begin{aligned} b_n(m,\, x) = &\left\{\left[mA_n(y) + \frac{n}{x}\right]J_{n+1/2}(x) - J_{n-1/2}(x)\right\} \\ &\times\left\{\left[mA_n(y) + \frac{n}{x}\right]\left[J_{n+1/2}(x) + (-1)^n jJ_{-n-1/2}(x)\right]\right. \\ &\left. - \left[J_{n-1/2}(x) - (-1)^n jJ_{-n+1/2}(x)\right]\right\}^{-1}. \end{aligned} \tag{A.10}$$

The Bessel functions of real argument which appear in (A.9) and (A.10) can be expressed with circular functions by defining following recursion formula;

$$w_n(x) = \frac{2n-1}{x}w_{n-1}(x) - w_{n-2}(x), \tag{A.11}$$

with

$$w_0(x) = \sin x - j\cos x = \sqrt{\frac{\pi x}{2}}[J_{1/2}(x) + jJ_{-1/2}(x)], \tag{A.12}$$

$$w_{-1}(x) = \cos x - j\sin x = \sqrt{\frac{\pi x}{2}}[J_{1/2}(x) - jJ_{1/2}(x)]. \tag{A.13}$$

For example,

$$w_1(x) = \frac{1}{x}w_0(x) - w_{-1}(x) = \sqrt{\frac{\pi x}{2}}[J_{3/2}(x) - jJ_{3/2}(x)], \tag{A.14}$$

$$w_2(x) = \frac{3}{x}w_1(x) - w_0(x) = \sqrt{\frac{\pi x}{2}}[J_{5/2}(x) + jJ_{5/2}(x)], \tag{A.15}$$

and $w_n(x)$ is generally expressed using finite term functions $J_{n+1/2}(x)$ and $J_{-n-1/2}(x)$ as

$$w_n(x) = \sqrt{\frac{\pi x}{2}}[J_{n+1/2}(x) + (-1)^n j J_{-n-1/2}(x)]. \tag{A.16}$$

Comparing (A.16) with (A.9) and (A.10), and eliminating $\sqrt{\frac{\pi x}{2}}$ which is common to the numerators and denominators, the Mie coefficients can be rewritten as

$$a_n(m,\, x) = \frac{\left[\dfrac{A_n(y)}{m} + \dfrac{n}{x}\right] \mathrm{Re}[w_n(x)] - \mathrm{Re}[w_{n-1}(x)]}{\left[\dfrac{A_n(y)}{m} + \dfrac{n}{x}\right] w_n(x) - w_{n-1}(x)}, \tag{A.17}$$

$$b_n(m,\, x) = \frac{\left[mA_n(y) + \dfrac{n}{x}\right] \mathrm{Re}[w_n(x)] - \mathrm{Re}[w_{n-1}(x)]}{\left[mA_n(y) + \dfrac{n}{x}\right] w_n(x) - w_{n-1}(x)}, \tag{A.18}$$

where $A_n(y)$ is arranged using the Riccati–Bessel functions in (A.3), and their derivatives (A.6) and (A.7) to lead the following equation

$$A_n(y) = \frac{J_{n-1/2}(y) - \dfrac{n}{y} J_{n+1/2}(y)}{J_{n+1/2}(y)} = -\frac{n}{y} + \frac{J_{n-1/2}(y)}{J_{n+1/2}(y)}. \tag{A.19}$$

If the above function is transformed into the following recursion formula:

$$\begin{aligned} A_n(y) &= -\frac{n-1}{y} + \frac{J_{n-3/2}(y)}{J_{n-1/2}(y)} \\ &= -\frac{n-1}{y} + \frac{\dfrac{2n-1}{y} J_{n-1/2}(y) - J_{n+1/2}(y)}{J_{n-1/2}(y)}, \end{aligned} \tag{A.20}$$

or

$$\frac{J_{n+1/2}(y)}{J_{n-1/2}(y)} = \frac{n}{y} - A_{n-1}(y). \tag{A.21}$$

Substituting (A.21) into (A.19), the final recursion formula of $A_n(y)$ can be expressed as

$$A_n(y) = -\frac{n}{y} + \left[\frac{n}{y} - A_{n-1}(y)\right]^{-1}, \tag{A.22}$$

and $A_0(y)$ becomes

$$A_0(y) = \frac{J_{-1/2}(y)}{J_{1/2}(y)} = \cot y. \tag{A.23}$$

Putting the real and imaginary parts of the complex refractive index be n_r and k_a, respectively, and $y \equiv mx = n_\mathrm{r}x - jk_\mathrm{a}x = p - jq$, where $p = n_\mathrm{r}x$ and $q = k_\mathrm{a}x$. Substituting these values into (A.23) and arranging the expression, $A_0(y)$ becomes

$$A_0(y) = \frac{\sin p \cos p + j \sinh q \cosh q}{\sin^2 p + \sinh^2 q}. \tag{A.24}$$

Using (A.22) and (A.24), actual $A_n(y)$ can be calculated. In addition, if m is real (nonabsorbing sphere), the imaginary parts of $A_0(y)$ and all $A_n(y)$ become 0.

Appendix B
Autocovariance Analysis

B.1 Mean Doppler Frequency

The autocorrelation function of a complex time series signal $R(\tau)$ is a complex number obtained by the inner product computation of complex signal and is expressed as

$$R(\tau) = A(\tau)\mathrm{e}^{j\theta(\tau)}, \tag{B.1}$$

where $A(\tau)$ denotes amplitude. As $R(\tau) = R(-\tau)^*$,

$$A(\tau) : \text{Real even } \ A(\tau) = A(-\tau), \tag{B.2}$$

$$\theta(\tau) : \text{Real odd } \ \theta(\tau) = -\theta(-\tau),\ \theta(0) = 0, \tag{B.3}$$

and the supersubscript * denotes complex conjugate. From Wiener–Khinchin's theorem, following relations are formed as shown in (5.86) and (5.87),

$$S(f) = \int_{-\infty}^{\infty} R(\tau)\mathrm{e}^{-j2\pi f\tau}\mathrm{d}\tau, \tag{B.4}$$

$$R(\tau) = \int_{-\infty}^{\infty} S(f)\mathrm{e}^{j2\pi f\tau}\mathrm{d}f. \tag{B.5}$$

Differentiating (B.5) with τ, and following relation is obtained,

$$\frac{\mathrm{d}R(\tau)}{\mathrm{d}\tau} = R'(\tau) = j2\pi\int_{-\infty}^{\infty} fS(f)\mathrm{e}^{j2\pi f\tau}\mathrm{d}f. \tag{B.6}$$

If $\tau = 0$, (B.5) and (B.6) become

$$R(0) = \int_{-\infty}^{\infty} S(f)\mathrm{d}f, \tag{B.7}$$

S. Fukao and K. Hamazu, *Radar for Meteorological and Atmospheric Observations*,
DOI 10.1007/978-4-431-54334-3, © Springer Japan 2014

$$R'(0) = j2\pi \int_{-\infty}^{\infty} fS(f)\mathrm{d}f, \tag{B.8}$$

respectively. $R(0)$ is the autocorrelation function (real) of time lag zero. From (5,107), Equations (B.7) and (B.8) are related with the first-order moment of power spectrum, $\mu_1 = E[f]$, as

$$\frac{R'(0)}{R(0)} = j2\pi E[f], \tag{B.9}$$

where $E[\,]$ denotes ensemble mean value. Differentiating (B.1) with τ,

$$R'(\tau) = A'(\tau)\mathrm{e}^{j\theta(\tau)} + jA(\tau)\mathrm{e}^{j\theta(\tau)}\theta'(\tau). \tag{B.10}$$

As $A(\tau)$ is an even function, $A'(0) = 0$ and $R'(0) = jA(0)\theta'(0)$. Hence, using $R(0) = A(0)$, (B.9) becomes

$$E[f] = \frac{\theta'(0)}{2\pi}. \tag{B.11}$$

If $\theta'(0)$ is approximated by the difference for the sample time interval T_s as

$$\theta'(0) \simeq \frac{\theta(T_\mathrm{s}) - \theta(0)}{T_\mathrm{s}} \tag{B.12}$$

and $\theta(0) = 0$ is applied, $E(f)$ becomes

$$E[f] \simeq \frac{\theta(T_\mathrm{s})}{2\pi T_\mathrm{s}}. \tag{B.13}$$

Now, $\theta(T_\mathrm{s})$ is the argument of the autocorrelation function $R(T_\mathrm{s})$, the mean Doppler frequency $\overline{f}$ is obtained by

$$\overline{f} = E[f] \simeq \frac{1}{2\pi T_\mathrm{s}} \arctan\left[\frac{\mathrm{I}_m[R(T_\mathrm{s})]}{\mathrm{R}_e[R(T_\mathrm{s})]}\right]. \tag{B.14}$$

B.2 Doppler Frequency Spectrum Width

From (5.108), second order derivative of $R(\tau)$, $R''(\tau)$, is related with the second order moment of power spectrum at $\tau = 0$ as

$$\frac{R''(0)}{R(0)} = -(2\pi)^2 E[f^2]. \tag{B.15}$$

The variance $\sigma_{f\mathrm{d}}^2$ of the mean Doppler frequency $E[f]$ is expressed as

$$\sigma_{f\mathrm{d}}^2 = E[f^2] - E[f]^2. \tag{B.16}$$

Substituting (B.9) and (B.15) into (B.16),

$$\sigma_{f\mathrm{d}}^2 = -\frac{1}{(2\pi)^2}\left[\frac{R''(0)}{R(0)} - \left(\frac{R'(0)}{R(0)}\right)^2\right] \tag{B.17}$$

is obtained. On the other hand, from (B.10),

$$\begin{aligned} R''(\tau) =& A''(\tau)\mathrm{e}^{j\theta(\tau)} + 2jA'(\tau)\mathrm{e}^{j\theta(\tau)}\theta'(\tau) \\ & - A(\tau)\mathrm{e}^{j\theta(\tau)}\theta'(\tau)^2 + jA(\tau)\mathrm{e}^{j\theta(\tau)}\theta''(\tau) \end{aligned} \tag{B.18}$$

is derived. As discussed previously, $A'(0) = 0$ and $R(0) = A(0)$, thus (B.18) becomes

$$\frac{R''(0)}{R(0)} = \frac{A''(0)}{A(0)} - \theta'(0)^2 + j\theta''(0). \tag{B.19}$$

Furthermore, from (B.9), (B.11), and (B.19),

$$\left(\frac{R'(0)}{R(0)}\right)^2 = -\theta'(0)^2 \tag{B.20}$$

is obtained. Substituting (B.19) and (B.20) into (B.17),

$$\sigma_{f\mathrm{d}}^2 = -\frac{1}{(2\pi)^2}\left[\frac{A''(0)}{A(0)} + j\theta''(0)\right] \tag{B.21}$$

is obtained.

The term $\theta''(0)$ in (B.21) can be assumed as the acceleration component of the Doppler velocity, thus if $\theta''(0)$ is approximated to $\theta''(0) \simeq 0$, (B.21) becomes

$$\sigma_{f\mathrm{d}}^2 \simeq -\frac{1}{(2\pi)^2}\frac{A''(0)}{A(0)}. \tag{B.22}$$

Using the Taylor series with center $= 0$ (the Maclaurin series of $A(T_\mathrm{s})$ for the sample time interval T_s around 0), we obtain

$$A(T_\mathrm{s}) = A(0) + T_\mathrm{s}\frac{\mathrm{d}A(0)}{\mathrm{d}\tau} + \frac{T_\mathrm{s}^2}{2}\frac{\mathrm{d}^2A(0)}{\mathrm{d}\tau^2} + \frac{T_\mathrm{s}^3}{6}\frac{\mathrm{d}^3A(0)}{\mathrm{d}\tau^3} + \cdots. \tag{B.23}$$

Neglecting the third and higher terms of (B.23) and accounting $A'(0) = 0$,

$$A(T_s) = A(0) + \frac{T_s^2}{2} A''(0), \tag{B.24}$$

and

$$\frac{A''(0)}{A(0)} = \frac{2}{T_s^2} \left[\frac{A(T_s)}{A(0)} - 1 \right]. \tag{B.25}$$

Substituting (B.25) into (B.22), we obtain

$$\sigma_{fd}^2 \simeq \frac{1}{2\pi^2 T_s^2} \left[1 - \frac{A(T_s)}{A(0)} \right]. \tag{B.26}$$

As $A(T_s)$ is the absolute value of $R(T_s)$, $R(0) = A(0)$, thus the squared Doppler frequency spectrum width (variance) is given by

$$\sigma_{fd}^2 \simeq \frac{1}{2\pi^2 T_s^2} \left[1 - \frac{|R(T_s)|}{R(0)} \right]. \tag{B.27}$$

Appendix C
The Fast Fourier Transform (FFT) Algorithm

C.1 Decimation-in-Time (DIT) FFT Algorithm

There are already a lot of documents about the high-speed calculation algorithm of the discrete Fourier transform (DFT). Here, we summarize the fast Fourier transform (FFT) based on Ziemer et al. (1998, Chap. 10) as follows. In the expression of discrete signals discussed in Sect. 5.5.3, the DFT is expressed from (5.121) as

$$V(k) = \sum_{m=0}^{M-1} v(m) W_M^{mk} \quad k = 0, 1, \cdots, M-1, \tag{C.1}$$

where

$$W_M = \mathrm{e}^{-j2\pi/M}. \tag{C.2}$$

For a discrete time signal series $v(m)$ of length M, the sum (C.1) gives a discrete Frequency signal series $V(k)$ of length M. If M is large such as several tens or several hundreds, number of operations according to (C.1) becomes huge as discussed in Sect. 8.4.4. Therefore, a great reduction of number of operations is desirable from the point of practical use.

The FFT is an algorithm to decrease the number of operations by limiting when length M becomes $M = 2^n$ (n: integer), and using the periodicity of (C.2). Consider the right-hand side (C.1) with the summation carried out separately over the even- and odd-index terms in the sum. If the indexes are $m = 2s$ for the even-index terms and $m = 2s+1$ for the odd-index terms, (C.1) is written as

$$\begin{aligned} V(k) &= \sum_{s=0}^{M/2-1} v(2s) W_M^{2sk} + \sum_{s=0}^{M/2-1} v(2s+1) W_M^{(2s+1)k} \\ &= \sum_{s=0}^{M/2-1} v(2s) W_M^{2sk} + W_M^k \sum_{s=0}^{M/2-1} v(2s+1) W_M^{2sk}. \end{aligned} \tag{C.3}$$

S. Fukao and K. Hamazu, *Radar for Meteorological and Atmospheric Observations*,
DOI 10.1007/978-4-431-54334-3, © Springer Japan 2014

Applying the relation

$$W_M^{2sk} = \mathrm{e}^{-j(2\pi/M)(2sk)} = \mathrm{e}^{-j[(2\pi)/(M/2)](sk)} = W_{M/2}^{sk}, \tag{C.4}$$

(C.3) becomes

$$\begin{aligned} V(k) &= \sum_{s=0}^{M/2-1} v(2s) W_{M/2}^{sk} + W_M^k \sum_{s=0}^{M/2-1} v(2s+1) W_{M/2}^{sk} \\ &= G(k) + W_M^k H(k) \quad k = 0, 1, \cdots, M-1, \end{aligned} \tag{C.5}$$

where $G(k)$ and $H(k)$ are

$$G(k) = \sum_{s=0}^{M/2-1} v(2s) W_{M/2}^{sk}, \tag{C.6}$$

$$H(k) = \sum_{s=0}^{M/2-1} v(2s+1) W_{M/2}^{sk}, \tag{C.7}$$

and are $(M/2)$-point DFT of the even- and odd-index points of the discrete time signal series $v(m)$, respectively. Since $G(k)$ and $H(k)$ are periodic in k with period $M/2$, only $M/2$ values of $G(k)$ and $H(k)$ are needed to compute (C.5). Assuming that an algorithm is available for computing an $(M/2)$-point DFT, the N-point DFT of $v(m)$ may be provided by combining the $(M/2)$-point DFTs, $G(k)$ and $H(k)$, in accordance with (C.5).

Figure C.1a shows the flow graph of the DIT decomposition for the DFT of $M = 8$, based on the combination of two $(M/2)$-point DFTs of the even- and odd-index points. In the figure, the lines with arrows indicate the quantities to be added, with the power of W_M along the arrow indicating the multiplication of $H(k)$ in (C.5) by W_M^k. Arrows with nothing beside them are multiplications by unity, i.e., the $G(k)$s are transmitted as they appear at the output of the DFT boxes, e.g., $V(0) = G(0) + W_M^0 H(0)$. Furthermore, we can break up each of the $M/2$-point DFTs in Panel (a) into two $M/4$-point DFTs, as shown in Fig. C.1(b), where the relation $W_{M/2}^s = W_M^{2s}$ is used in combining the sums $G(k)$ and $H(k)$. The same procedure can be continued until a series of $M/2$-point DFTs results for the first stage of the M-point DFT computation. Figure C.2 shows the procedure to the final stage for $M = 8$, which is a precise flow graph of the FFT. Since this algorithm separates the input time signal samples into successively smaller sets, the resulting algorithm is referred as a decimation-in-time (DIT) FFT. The schematic of W_M^k for $M = 8$ is shown in Fig. C.3, and 2-point DFT flow graph is shown in Fig. C.4.

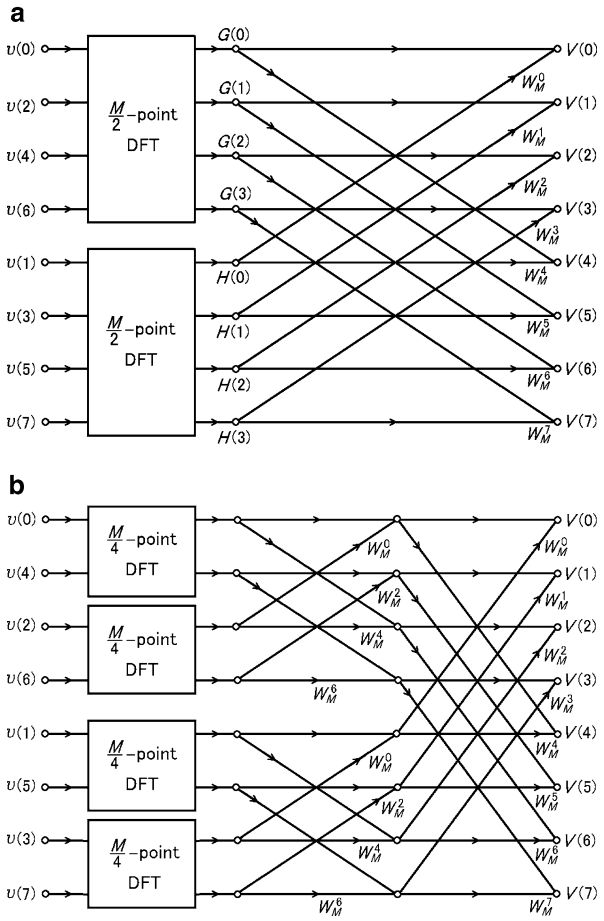

Fig. C.1 Flow graph of the DIT decomposition for the DFT of $M = 8$, based on the combination of (**a**) two $(M/2)$-point DFTs of the even- and odd-index points and (**b**) that of four $(M/4)$-point DFTs

C.2 Decimation-in-Frequency (DIF) FFT Algorithm

Here we discuss another type of algorithm for finding the DFT. Consider the DFT sum (C.1) with the sum carried out over the first half and the last half of the input ample separately, the result becomes

$$\begin{aligned} V(k) &= \sum_{m=0}^{M/2-1} v(m) W_M^{mk} + \sum_{m=M/2}^{M-1} v(m) W_M^{mk} \\ &= \sum_{m=0}^{M/2-1} v(m) W_M^{mk} + W_M^{(M/2)k} \sum_{m=0}^{M/2-1} v\left(m + \frac{M}{2}\right) W_M^{mk}. \end{aligned} \tag{C.8}$$

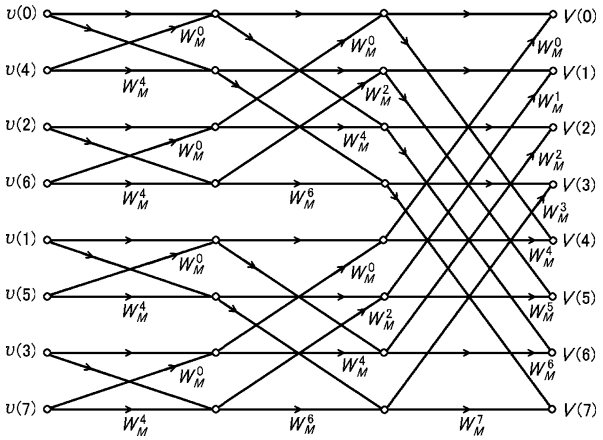

Fig. C.2 Procedure to the final stage for $M = 8$, which is a precise flow graph of the FFT

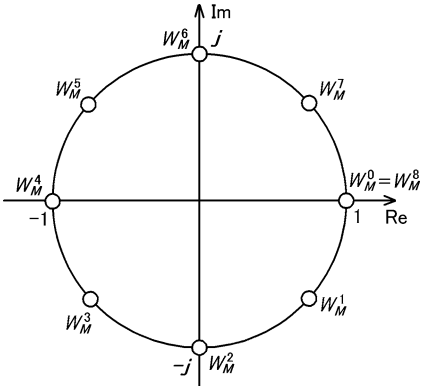

Fig. C.3 Schematic of W_M^k for $M = 8$

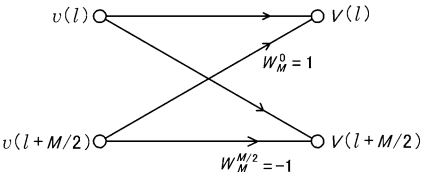

Fig. C.4 Flow graph of 2-point DFT, $M = 2$

Using the fact that $W_M^{(M/2)k} = (-1)^k$ to combine the two sums in (C.8), and we obtain

$$V(k) = \sum_{m=0}^{M/2-1} \left[v(m) + (-1)^k v\left(m + \frac{M}{2}\right) W_M^{mk} \right]. \tag{C.9}$$

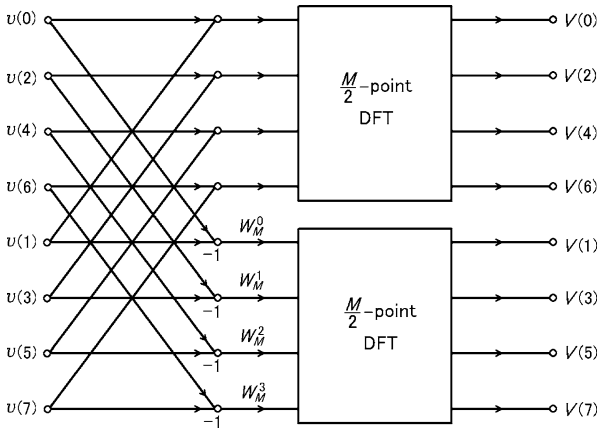

Fig. C.5 Flow graph for the first separation to two $(M/2)$-point DFTs of 8-point DFT in the DIF FFT algorithm

If k is treated even and odd separately as $k = 2s$ and $k = 2s+1$, respectively, the even- and odd-index output points of (C.9) are indicated for $s = 0, 1, \cdots, M/2-1$ as

$$V(2s) = \sum_{m=0}^{M/2-1} \left[v(m) + v\left(m + \frac{M}{2}\right) \right] W_M^{2sm}, \tag{C.10}$$

$$V(2s+1) = \sum_{m=0}^{M/2-1} \left[v(m) - v\left(m + \frac{M}{2}\right) \right] W_M^{m} W_M^{2sm}. \tag{C.11}$$

Since $W_M^{2m} = W_{M/2}^{m}$ as noted previously, (C.10) and (C.11) are both $M/2$-point DFTs. The flow graph for obtaining $V(k)$ in this fashion is shown in Fig. C.5. This process can be expanded to replace each $(M/2)$-point DFT by two $(M/4)$-point DFTs, and so on until only two points are left in each DFT. The final flow graph for 8-point DFT becomes precisely the reverse of Fig. C.2, with all arrows reversed and input and output interchanged. Since the frequency points were subdivided to obtain this algorithm, it is called as a decimation-in-frequency (DIF) FFT algorithm.

Appendix D
Radar Equation for RASS Echo

The radar equation for the radio acoustic sounding system (RASS) was first given by Marshall et al. (1972). Clifford and Wang (1977) discuss the equation based on them. The following discussion are based on Clifford and Wang.

Assuming that both radar antenna and acoustic wave source are at the origin of coordinates, and that the radar range resolution and the beam width are ΔR and $2\theta_{\mathrm{r}}$, respectively as shown in Fig. D.1, a volume element dv at (r, ϕ, θ) in the sampling volume scatters the radar waves and generates a RASS echo at $(r_0, \phi_0, \pi/2)$. The electric field at the point $\boldsymbol{r_0}$ in the xy-plane generated by the RASS echo is derived as follows.

The electric field generated at $\boldsymbol{r_0}$ due to the refractive index perturbations $\Delta n(\boldsymbol{r})$ is expressed by the volume integration of the electric field $E(\boldsymbol{r})$ and $\Delta n(\boldsymbol{r})$ in the scattering volume as

$$E_{\mathrm{r}}(\boldsymbol{r_0}) = \frac{k^2}{2\pi} \int_V \frac{\exp(jk|\boldsymbol{r_0} - \boldsymbol{r}|)}{|\boldsymbol{r_0} - \boldsymbol{r}|} \Delta n(\boldsymbol{r}) E(\boldsymbol{r}) \mathrm{d}v, \tag{D.1}$$

where k is the radar wavelength. Using the transmission electric field E_0, $E(r)$ can be expressed as

$$E(r) = \frac{E_0}{r} \exp(jkr), \tag{D.2}$$

whereas the refractive index perturbation $\Delta n(r)$ of a sine acoustic wave becomes

$$\Delta n(r) = \begin{cases} \dfrac{A_{\mathrm{a}}}{r} \exp(jk_{\mathrm{a}} r) & R - \Delta R/2 < r < R + \Delta R/2, \\ 0 & \text{otherwise}, \end{cases} \tag{D.3}$$

where A_{a} is a constant given by (7.89) and is determined by characteristics of sound source and condition of the atmosphere, and k_{a} is the wavenumber of the acoustic wave.

S. Fukao and K. Hamazu, *Radar for Meteorological and Atmospheric Observations*,
DOI 10.1007/978-4-431-54334-3, © Springer Japan 2014

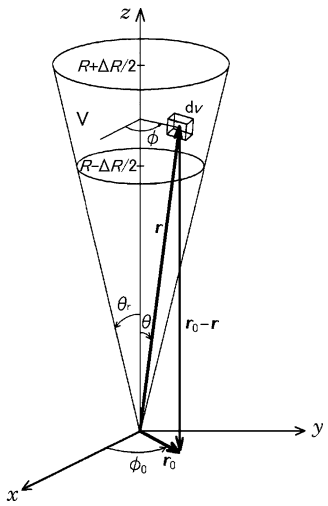

Fig. D.1 Geometric configuration for a radar equation of RASS echo. Both radar antenna and acoustic wave sources are located at the origin and transmit the waves to the zenith. The radar range resolution and the beam width are ΔR and $2\theta_\mathrm{r}$, respectively. A volume element dv at (r, ϕ, θ) in the sampling volume scatters the radar waves and generate a RASS echo at $(r_0, \phi_0, \pi/2)$ [from Marshall et al. 1972]

For simplicity, put the denominator $|\boldsymbol{r_0} - \boldsymbol{r}|$ of (D.1) as $|\boldsymbol{r_0} - \boldsymbol{r}| = R$ and approximate the numerator $|\boldsymbol{r_0} - \boldsymbol{r}|$ as

$$|\boldsymbol{r_0} - \boldsymbol{r}| = r - r_0 \sin\theta \cos(\phi - \phi_0). \tag{D.4}$$

As the RASS echo extends isotropically in the azimuthal direction, the value $|\boldsymbol{r_0} - \boldsymbol{r}|$ is represented by the value for $\phi_0 = 0$, thus (D.4) is replaced with

$$|\boldsymbol{r_0} - \boldsymbol{r}| = r - r_0 \sin\theta \cos\phi. \tag{D.5}$$

From Fig. D.1, dv is expressed in the polar coordinate as

$$\mathrm{d}v = r^2 \sin\theta \mathrm{d}\theta \mathrm{d}\phi \mathrm{d}r. \tag{D.6}$$

Substituting these equations into (D.1), and

$$\begin{aligned} E_\mathrm{r}(\boldsymbol{r_0}) = & \frac{k^2 E_0 A_\mathrm{a}}{2\pi R} \int_0^{\theta_\mathrm{r}} \sin\theta \mathrm{d}\theta \int_0^{2\pi} \exp[jk(-r_0 \sin\theta \cos\phi)] \mathrm{d}\phi \\ & \times \int_{R-\Delta R/2}^{R+\Delta R/2} \exp[j(2k + k_\mathrm{a})r] \mathrm{d}r. \end{aligned} \tag{D.7}$$

Applying that $\sin\theta \simeq \theta$ if $\theta \ll 1$, (D.7) is expressed as

$$\begin{aligned} E_\mathrm{r}(\boldsymbol{r_0}) &= \frac{k^2 E_0 A_\mathrm{a}}{2\pi R} 2\pi \int_0^{\theta_\mathrm{r}} \theta J_0(kr_0\theta) \mathrm{d}\theta \int_{R-\Delta R/2}^{R+\Delta R/2} \exp[j(2k + k_\mathrm{a})r] \mathrm{d}r \\ &= \frac{k^2 E_0 A_\mathrm{a}}{2\pi R} (\pi\theta_\mathrm{r}^2) \frac{2J_1(kr_0\theta_\mathrm{r})}{kr_0\theta_\mathrm{r}} \int_{R-\Delta R/2}^{R+\Delta R/2} \exp[j(2k + k_\mathrm{a})r] \mathrm{d}r, \end{aligned} \tag{D.8}$$

where $J_0(kr_0\theta)$ and $J_1(kr_0\theta_r)$ are 0th and 1th Bessel function of the first kind, respectively. $2J_1(kr_0\theta_r)/kr_0\theta_r$ in the right-hand side of (D.8) shows the radiation pattern of the radar antenna that generates the electromagnetic wave of beam width of $2\theta_r$. In the RASS method, the same antenna is used for transmission and reception of radar waves, thus the received power of RASS echo P_{ar} is given by

$$P_{ar} = \int_0^{r_e} \int_0^{2\pi} \frac{|E_r(r_0)|^2}{Z_0} r_0 \mathrm{d}r_0 \mathrm{d}\phi_0, \tag{D.9}$$

where r_e and Z_0 are the radius of radar antenna and its characteristic impedance, respectively. Substituting (D.8) into (D.9), P_{ar} becomes

$$P_{ar} = \frac{1}{Z_0}\left(\frac{k^2 E_0 A_a}{2R}\theta_r^2\right)^2 \int_0^{2\pi} \mathrm{d}\phi_0 \int_0^{r_e} \left[\frac{2J_1(kr_0\theta_r)}{kr_0\theta_r}\right]^2 r_0 \mathrm{d}r_0 \times \left\{\int_{R-\Delta R/2}^{R+\Delta R/2} \exp[j(2k+k_a)r]\mathrm{d}r\right\}^2. \tag{D.10}$$

The integration for ϕ_0 and r_0 in the right-hand side of (D.10) expresses the maximum value of the radar cross section, and can be calculated by assuming that the effective antenna aperture is infinite as

$$\int_0^{2\pi} \mathrm{d}\phi_0 \int_0^{\infty} \left[\frac{2J_1(kr_0\theta_r)}{kr_0\theta_r}\right]^2 r_0 \mathrm{d}r_0 = \frac{4\pi}{(k\theta_r)^2} \tag{D.11}$$

$$= g\frac{\lambda^2}{4\pi}, \tag{D.12}$$

where g and λ are the antenna gain and the wavelength of the radar, respectively. The transmission electric field E_0 and the transmitted peak power P_t are related as

$$\frac{E_0^2}{Z_0 R^2} = \frac{P_t g}{4\pi R^2}. \tag{D.13}$$

Substituting (D.11)–(D.13) into (D.10), and P_{ar} becomes

$$P_{ar} = A_a^2 \frac{4\pi^2 P_t}{\lambda^2 R^2}\left\{\int_{R-\Delta R/2}^{R+\Delta R/2} \exp[j(2k+k_a)r]\mathrm{d}r\right\}^2. \tag{D.14}$$

The integration of the right-hand side of (D.14) is

$$\int_{R-\Delta R/2}^{R+\Delta R/2} \exp[j(2k+k_a)r]\mathrm{d}r = \frac{\Delta R}{2}\left\{\cos[(2k+k_a)R]\mathrm{sinc}\left[(2k+k_a)\frac{\Delta R}{2}\right] + \cos[(2k-k_a)R]\mathrm{sinc}\left[(2k-k_a)\frac{\Delta R}{2}\right]\right\}, \tag{D.15}$$

where $\mathrm{sinc}x = \sin x/x$. If $2k \simeq k_\mathrm{a}$, $\mathrm{sinc}[(2k+k_\mathrm{a})\Delta R/2]$ becomes small, thus the term that include $2k+k_\mathrm{a}$ in the right-hand side of (D.15) becomes negligible, and (D.15) is simplified as

$$\int_{R-\Delta R/2}^{R+\Delta R/2} \exp[j(2k+k_\mathrm{a})r]\mathrm{d}r = \frac{\Delta R}{2}\mathrm{sinc}\left[(2k-k_\mathrm{a})\frac{\Delta R}{2}\right]. \tag{D.16}$$

Substituting (D.16) into (D.14), the radar equation for the RASS echo is expressed as

$$P_\mathrm{ar} = A_\mathrm{a}^2 \frac{4\pi^2 P_\mathrm{t}}{\lambda^2 R^2}\left(\frac{\Delta R}{2}\right)^2 \mathrm{sinc}^2\left[(2k-k_\mathrm{a})\frac{\Delta R}{2}\right]. \tag{D.17}$$

It is obvious from (D.17) that the received power of the RASS echo is proportional to the square of the range resolution of the radar and inverse proportional to the square of the distance from the radar. Replacing R with r and ΔR with Δr, respectively in (D.17), (7.90) is obtained.

References

Adachi, T. 1996. *Detailed temperature structure of meteorological disturbances observed with RASS (Radio Acoustic Sounding System)*, 173 pp. Ph.D. dissertation. Kyoto University.

Alexander, S., T. Tsuda, J. Furumoto, T. Shimomai, T. Kozu, and M. Kawashima. 2006. A statistical overview of convection during the CPEA-I campaign. *Journal of the Meteorological Society of Japan* 84: 57–93.

Alvarez, H., J. Aparici, J. May, and F. Olmos. 1997. A 45-MHz continuum survey of the southern hemisphere. *Astronomy and Astrophysics Supplement Series* 124: 315–328.

Armijo, L. 1969. A theory for the determination of wind and precipitation velocities with Doppler radars. *Journal of the Atmospheric Sciences* 26: 570–573.

Atlas, D. and C.W. Ulbrich. 1977. Path- and area-integrated rainfall measurement by microwave attenuation in 1–3 cm band. *Journal of Applied Meteorology* 16: 1322–1331.

Atlas, D., R.S. Srivastava, and R.S. Sekhon. 1973. Doppler radar characteristics of precipitation at vertical incidence. *Reviews of Geophysics and Space Physics* 11: 1–35.

Balsley, B.B., and W.L. Ecklund. 1972. A portable coaxial collinear antenna. *IEEE Transactions on Antennas and Propagation* AP-20: 512–516.

Balsley, B.B., and K.S. Gage. 1980. The MST radar technique: Potential for middle atmospheric studies. *Pure and Applied Geophysics* 118: 452–493.

Balsley, B.B., W.L. Ecklund, D.A. Carter, and P.E. Johnston. 1980. The MST radar at Poker Flat, Alaska. *Radio Science* 15: 213–223.

Barratt, P. and I. C. Browne. 1953. A new method of measuring vertical air currents. *Quart. J. Roy. Meteor. Soc.* 79: 550.

Battan, L.J. 1973. *Radar observation of the atmosphere*, 324 pp. Illinois: The University of Chicago Press.

Bean, B.R., and E.J. Dutton. 1966. *Radio meteorology*. National Bureau of Standards, Monograph 92, Supt. Doc. U.S. Govt., Printing Office, Washington.

Beard, K.V., and C. Chuang. 1987. A new model for the equilibrium shape of raindrops. *Journal of the Atmospheric Sciences* 44: 1509–1524.

Benoit, A. 1968. Signal attenuation due to neutral oxygen and water vapor, rain and clouds. *Microwave Journal* 11: 73–80.

Berger, T., and H.L. Groginsky. 1973. Estimation of the spectral moments of pulse trains. In *International conference on information theory (preprints)*, Tel Aviv, Israel.

Bienvenu, G., L. Kopp. 1983. Optimality of high resolution array processing using the eigensystem approach. *IEEE Transactions on Acoustics, Speech, & Signal Processing* 31: 1235–1248.

Biggerstaff, M.I., and R.A. Houze, Jr. 1993. Kinematics and microphysics of the transition zone of the 10–11 June 1985 squall line. *Journal of the Atmospheric Sciences* 50: 3091–3110.

Booker, H.G., and W.E. Gordon. 1950. A theory of radio scattering in the troposphere. *Proceedings of the IRE* 38: 401–412.

S. Fukao and K. Hamazu, *Radar for Meteorological and Atmospheric Observations*,
DOI 10.1007/978-4-431-54334-3, © Springer Japan 2014

Borgeaud, M., R.T. Shin, and J.A. Kong. 1987. Theoretical models for polarimetric radar clutter. *Journal of Electromagnetic Waves and Applications* 1: 73–89

Brandes, E.A. 1977. Flow in severe thunderstorms observed by dual-Doppler radar. *Monthly Weather Review* 105: 113–120.

Briggs, B.H. 1984. The analysis of spaced sensor records by correlation technique. In *Handbook for MAP*, vol. 13, 166–186. Urbana: ICSU Scientific Committee on Solar-Terrestrial Physics (SCOSTEP).

Briggs, B.H., and R.A. Vincent. 1992. Spaced-antenna analysis in the frequency domain. *Radio Science* 27: 117–129.

Bringi, V.N., and V. Chandrasekar. 2001. *Polarimetric Doppler weather radar*, 636 pp. New York: Cambridge University Press.

Bringi, V.N., R. Hoferer, D.A. Brunkow, R. Schwerdtfeger, V. Chandrasekar, S.A. Rutledge, J. George, and P.C. Kennedy. 2011. Design and performance characteristics of the new 8.5-m dual-offset Gregorian antenna for the CSU-CHILL radar. *Journal of Atmospheric and Oceanic Technology* 28: 907–920.

Browning, K.A. 1986. Conceptual models of precipitation systems. *Weather and Forecasting* 1: 23–41.

Browning, K.A., and G.A. Monk. 1982. A simple model for the synoptic analysis of cold fronts. *Quarterly Journal of the Royal Meteorological Society* 108: 435–452.

Browning, K.A., and R. Wexler. 1968. A determination of kinematic properties of a wind field using Doppler radar. *Journal of Applied Meteorology* 7: 105–113.

Browning, K.A., J.C. Fankhauser, J.P. Chalon, P.J. Eccles, R.G. Strauch, F.H. Merrem, D.J. Musil, E.L. May, and W.R. Sand. 1976. Structure of an evolving hailstorm, Part V: Synthesis and implications for hail growth and hail suppression. *Monthly Weather Review* 104: 603–610.

Capon, J. 1969. High-resolution frequency-wavenumber spectrum analysis. *Proceedings of the IEEE* 57: 1408–1418.

Caughey, S.J., B.A. Crease, D.N. Asimakapoulos, and R.S. Cole. 1978. Quantitative bistatic acoustic sounding of the atmospheric boundary layer. *Quarterly Journal of the Royal Meteorological Society* 104: 146–161.

CCIR. 1991. CCIR, Propagation data and prediction methods required for terrestrial line-of-site systems, CCIR Reports 338-6, V, ITU, Geneva, 1991.

Cheong, B.L., M.W. Hoffman, R.D. Palmer, S.J. Fraiser, and F.J. López-Dekker. 2004. Pulse pair beamforming and the effects of reflectivity field variations on imaging radars. *Radio Science* 39:RS3014. doi:10.1029/2002RS002843.

Cheong, B.L., M.W. Hoffman, R.D. Palmer, S.J. Frasier, and F.J. López-Dekker. 2006. Phased-array design for biological clutter rejection : Simulation and experimental validation. *Journal of Atmospheric and Oceanic Technology* 23: 585–598.

Cheong, B.L., T.-Y. Yu, R.D. Palmer, K.-F. Yang, M.W. Hoffman, S.J. Frasier, and F.J. Lopez-Dekker. 2008. Effects of wind wield inhomogeneities on Doppler beam swinging received by an imaging radar. *Journal of Atmospheric and Oceanic Technology* 25: 1414–1422.

Chilson, P.B., T.Y. Yu, R.G. Strauch, A. Muscinski, and R.D. Palmer. 2003. Implementation and validation of range imaging on a UHF radar wind profiler. *Journal of Atmospheric and Oceanic Technology* 104: 987–996.

Cho, J.Y.N. 2009. Moving clutter spectral filter for terminal Doppler weather radar. In *34th International conference on radar meteorology (preprints)*. Williamsburg: American Meteorological Society, P5.2.

Clifford, S.F., and T.I. Wang. 1977. The range limitation on radar-acoustic sounding system (RASS) due to atmospheric refractive turbulence. *IEEE Transactions on Antennas and Propagation* 25: 319–326.

Cohn, S. 1995. Radar measurements of turbulent eddy dissipation rate in the troposphere: A comparison of techniques. *Journal of Atmospheric and Oceanic Technology* 12: 85–95.

Cole, A.E., A. Court, and A.J. Kantor. 1965. Model atmospheres, In *Handbook of geophysics and space environment*, ed. S.L. Valley. Bedford: Office of Aerospace Research, USAF, Cambridge Research Laboratories, Chapter 2.

Cooley, J.W., and J.W. Tukey. 1965. An algorithm for the machine calculation of complex Fourier series. *Mathematics of Computation* 19: 297–301.

Costa, E., and F. Fougere. 1988. Cross-spectral analysis of spaced-receiver measurements. *Radio Science* 23: 129–139.

Crane, R.K. 1980. A review of radar observations of turbulence in the lower stratosphere. *Radio Science* 15: 177–193.

Crocker, S.C. 1988. *TDWR PRF selection criteria*, 57 pp. Project Rep. ATC-147, DOT/FAA/PM-87-25, MIT Lincoln Laboratory.

Czechowsky, P., G. Schmidt, and R. Rüster. 1984. The mobile SOUSY Doppler radar: Technical design and first results. *Radio Science* 19: 441–450.

Dalaudier, F., C. Sidi, M. Crochet, and J. Vernin. 1994. Direct evidence of "sheet" in the atmospheric temperature field. *Journal of the Atmospheric Sciences* 51: 237–248.

Davies-Jones, R.P. 1979. Dual-Doppler coverage area as a function of measurement accuracy and spatial resolution. *Journal of Applied Meteorology* 18: 1229–1233.

de Elía, R., and I. Zawadzki. 2000. Sidelobe contamination in bistatic radars. *Journal of Atmospheric and Oceanic Technology* 17: 1313–1329.

de Elía, R., and I. Zawadzki. 2001. Optimal layout of a bistatic radar network. *Journal of Atmospheric and Oceanic Technology* 18: 1184–1194.

Deirmendjian, D. 1969. *Electromagnetic scattering on spherical polydispersions*, 290 pp. New York: Elsevier.

Dhaka, S.K., M. Takahashi, Y. Kawatani, S. Malik, Y. Shibagaki, and S. Fukao. 2003. Observations of deep convective updrafts in tropical convection and their role in the generation of gravity waves. *Journal of the Meteorological Society of Japan* 81: 1185–1199.

Dhaka, S.K., M.K. Yamamoto, Y. Shibagaki, H. Hashiguchi, S. Fukao, and H.-Y. Chun. 2006. Equatorial Atmosphere Radar observations of short vertical wavelength gravity waves in the upper troposphere and lower stratosphere region induced by localized convection. *Geophysical Research Letters* 33: L19805. doi:10.1029/2006GL027026.

Dicke, R.H. 1946. The measurement of thermal radiation at microwave frequencies. *Review of Scientific Instruments* 17: 268–275.

Doviak, R.J. 1972. Comparison of bistatic and monostatic radar detection of clear air atmospheric targets. *AIAA paper*, 8 pp. No. 72–175, Copies available from AIAA library, 750 3rd Ave., New Yoke, NY 10017.

Doviak, R.J., and R.D. Palmer. 2014. Polarimetric doppler weather radar. In *Encyclopedia of atmospheric science*, ed. G. North. 2nd ed. London: Elsevier.

Doviak, R.J., and P.S. Ray. 1976. Error estimation in wind fields derived from dual-Doppler radar measurement. *Journal of Applied Meteorology* 15: 868–878.

Doviak, R.J., and C.M. Weil. 1972. Bistatic radar detection of the melting layer. *Journal of Applied Meteorology* 11: 1012–1016.

Doviak, R.J., and D.S. Zrnić. 1984. *Doppler radar and weather observations*, 458 pp. Orlando: Academic.

Doviak, R.J., and D.S. Zrnić. 2006. *Doppler radar and weather observations*, 562 pp. 2nd ed. Mineola: Dover.

Doviak, R.J., J. Goldhirsh, and A.R. Miller. 1972. Bistatic-radar detection of high-altitude clear-air atmospheric targets. *Radio Science* 7: 993–1003.

Doviak, R.J., R.J. Lataitis, and C.L. Holloway. 1996. Cross correlations and cross spectra for spaced antenna wind profilers 1. Theoretical analysis. *Radio Science* 31: 157–180.

Doviak, R.J., V. Bringi, A. Ryzhkov, A. Zahrai, and D. Zrnić. 2000. Considerations for polarimetric upgrades to operational WSR-88D radars. *Journal of Atmospheric and Oceanic Technology* 17: 257–278.

Droegemeier, K.K., and R.B. Wilhelmson. 1987. Numerical simulation of thunderstorm outflow dynamics, Part I: Outflow sensitivity experiments and turbulence dynamics. *Journal of the Atmospheric Sciences* 44: 1180–1210.

Easterbrook, C.C. 1974. Estimating horizontal wind fields by two-dimensional curve fitting of single Doppler radar measurements. In *16th Conference on radar meteorology (preprints)*, 214–219. Boston: American Meteorological Society.

Ecklund, W.L., D.A. Carter, and B.B. Balsley. 1988. A UHF wind profiler for the boundary layer: Brief description and initial results. *Journal of Atmospheric and Oceanic Technology* 5: 432–441.

Einaudi, F., D.P. Lalas, and G.E. Perona. 1978. The role of gravity waves in tropospheric processes. *Pure and Applied Geophysics* 117: 627–663.

Evans, J.V. 1969. Theory and practice of troposphere study by Thomson scatter radar. *Proceedings of the IEEE* 57: 496–500.

Fang, M., and R.J. Doviak. 2008. Coupled contributions in the Doppler radar spectrum width equation. *Journal of Atmospheric and Oceanic Technology* 25: 2245–2258.

Fang, M., R.J. Doviak, and V. Melnikov. 2004. Spectrum width measured by WSR-88D: Error sources and statistics of various weather phenomena. *Journal of Atmospheric and Oceanic Technology* 21: 888–904.

Fang, M., R.J. Doviak, and B.A. Albrecht. 2012. Analytical expressions for Doppler spectra of scatter from hydrometeors observed with a vertically directed radar beam. *Journal of Atmospheric and Oceanic Technology* 29: 500–509.

Farley, D., H. Ierkic, and B. Fejer. 1981. Radar interferometry: A new technique for studying plasma turbulence in the ionosphere. *Journal of Geophysical Research* 86: 1467–1472.

Franke, S.J. 1990. Pulse compression and frequency domain interferometry with a frequency-hopped MST radar. *Radio Science* 25: 565–574.

Fraser, G.J. 1968. Seasonal variation of southern hemisphere mid-latitude winds at altitudes of 70–100 km. *Journal of Atmospheric and Terrestrial Physics* 30: 707–720.

Friend, A.W. 1949. Theory and practice of tropospheric sounding by radar. *Proceedings of the IRE* 37: 116–138.

Fritts, D.C. 1984. Shear excitation of atmospheric gravity waves, 2. Nonlinear radiation from a free shear layer. *Journal of the Atmospheric Sciences* 41: 524–537.

Fritts, D.C., and Z. Luo. 1992. Gravity wave excitation by geostrophic adjustment of the jet stream, Part 1: Two-dimensional forcing. *Journal of the Atmospheric Sciences* 49: 681–697.

Fritts, D.C., and G.D. Nastrom. 1992. Sources of mesoscale variability of gravity waves, Part 2: Frontal, convective and jet stream excitation. *Journal of the Atmospheric Sciences* 49: 111–127.

Fujita, T.T. 1985. *The downburst: Microburst and macroburst, SMRP Res. Rep.* 210, 122 pp. Chicago: University of Chicago.

Fujita, T.T., and J. McCarthy. 1990. The application of weather radar to aviation meteorology. In *Radar in meteorology*, ed. D. Atlas, 657–681. Boston: American Meteorological Society.

Fujiwara, M., M.K. Yamamoto, H. Hashiguchi, T. Horinouchi, and S. Fukao. 2003. Turbulence at the tropopause due to breaking Kelvin waves observed by the Equatorial Atmosphere Radar. *Geophysical Research Letters* 30: 1171. doi:10.1029/2002GL01627.

Fujiyoshi, Y. 2001. Three dimensional radar echo structure of a vortex-like disturbance developed in a strong horizontal wind shear zone. *Tenki, Meteorological Society of Japan* 48: 3–4 (in Japanese).

Fujiyoshi, Y., and B. Geng. 1995. Dual Doppler radar observation of a tropical rainband developed from two convective clouds. *Journal of the Meteorological Society of Japan* 73: 471–490.

Fujiyoshi, Y., N. Yoshimoto, and T. Takeda. 1998. A dual-Doppler radar study of longitudinal-mode snowbands, Part I: A three dimensional kinematic structure of meso-γ-scale convective cloud systems within a longitudinal-mode snowband. *Monthly Weather Review* 126: 72–91.

Fukao, S. 2006. Coupling processes in the equatorial atmosphere (CPEA): A project overview. *Journal of the Meteorological Society of Japan* 84: 1–18.

Fukao, S., and R.D. Palmer. 1991. Spatial and frequency domain interferometry using the MU radar: A tutorial and recent developments. *Journal of Geomagnetism and Geoelectricity* 43: 645–666.

Fukao, S., T. Sato, S. Kato, R.M. Harper, R.F. Woodman, and W.E. Gordon. 1979. Mesospheric winds and waves over Jicamarca on May 23–24. *Journal of Geophysical Research* 84: 4379–4386.

Fukao, S., S. Kato, T. Aso, M. Sasada, and T. Makihira. 1980a: Middle and upper atmosphere radar (MUR) under design in Japan. *Radio Science* 15: 225–231.

Fukao, S., K. Wakasugi, and S. Kato. 1980b. Radar measurement of short-period atmospheric waves and related scattering properties at the altitude of 13–25 km over Jicamarca. *Radio Science* 15: 431–438.

Fukao, S., T. Sato, T. Tsuda, S. Kato, K. Wakasugi, and T. Makihira. 1985a. The MU radar with an active phased array system: 1. Antenna and power amplifiers. *Radio Science* 20: 1155–1168.

Fukao, S., T. Tsuda, T. Sato, S. Kato, K. Wakasugi, and T. Makihira. 1985b. The MU radar with an active phased array system: 2. In-house equipment. *Radio Science* 20: 1169–1176.

Fukao, S., T. Sato, and S. Kato. 1985c. Monitoring of the MU radar antenna pattern by satellite OHZORA (EXOS-C). *Journal of Geomagnetism and Geoelectricity* 37: 431–441.

Fukao, S., K. Wakasugi, T. Sato, T. Tsuda, I. Kimura, N. Takeuchi, M. Matsuo, and S. Kato. 1985d. Simultaneous observation of precipitating atmosphere by VHF band and C/Ku band radars. *Radio Science* 20: 622–630.

Fukao, S., K. Wakasugi, T. Sato, S. Morimoto, T. Tsuda, I. Hirota, I. Kimura, and S. Kato. 1985e. Direct measurement of air and precipitation particle motion by very high frequency Doppler radar. *Nature* 316: 712–714.

Fukao, S., T. Sato, H. Hojo, I. Kimura, and S. Kato. 1986. A numerical consideration on edge effect of planar dipole phased arrays. *Radio Science* 21: 1–12.

Fukao, S., T. Sato, T. Tsuda, S. Kato, M. Inaba, and I. Kimura. 1988a. VHF Doppler radar determination of the momentum flux in the upper troposphere and lower stratosphere: Comparison between the three- and four-beam methods. *Journal of Atmospheric and Oceanic Technology* 5: 57–69.

Fukao, S., M. Inaba, I. Kimura, T. Sato, T. Tsuda, and S. Kato. 1988b. A systematic error in MST/ST radar measurement induced due to finite range volume effect: 2. Numerical considerations. *Radio Science* 23: 74–82.

Fukao, S., M.D. Yamanaka, H. Matsumoto, T. Sato, T. Tsuda, and S. Kato. 1989. Wind fluctuations near a cold vortex-tropopause funnel system observed by the MU radar. *Pure and Applied Geophysics* 130: 463–479.

Fukao, S., T. Sato, T. Tsuda, M. Yamamoto, M.D. Yamanaka, and S. Kato. 1990. MU radar: New capabilities and system calibrations. *Radio Science* 25: 477–485.

Fukao, S., M.C. Kelley, T. Shirakawa, T. Takami, M. Yamamoto, T. Tsuda, and S. Kato. 1991. Turbulent upwelling of the mid-latitude ionosphere: 1. Observational results by the MU radar. *Journal of Geophysical Research* 96: 3725–3746.

Fukao, S., N. Ao, M.D. Yamanaka, W.K. Hocking, T. Sato, M. Yamamoto, T. Nakamura, T. Tsuda, and S. Kato. 1994. Seasonal variability of vertical eddy diffusivity in the middle atmosphere I: Three-year observations by the MU radar. *Journal of Geophysical Research* 99: 18973–18987.

Fukao, S., H. Hashiguchi, M. Yamamoto, T. Tsuda, T. Nakamura, M. K. Yamamoto, T. Sato, M. Hagio, and Y. Yabugaki. 2003. Equatorial Atmosphere Radar (EAR): System description and first results. *Radio Science* 38: 1053. doi:10.1029/2002RS002767.

Furumoto, J. 2002. *Observation of turbulence echo characteristics and humidity profiles with the MU radar-RASS*, 134 pp. Ph.D. dissertation. Kyoto University.

Furumoto, J., K. Kurimoto, and T. Tsuda. 2003. Continuous observations of humidity profiles with the MU radar-RASS combined with GPS and rawinsonde measurements. *Journal of Atmospheric and Oceanic Technology* 20: 23–41.

Furumoto, J., T. Tsuda, S, Iwai, T, Kozu. 2006. Continuous humidity monitoring in a tropical region with the equatorial atmosphere radar. *Journal of Atmospheric and Oceanic Technology* 23: 538–551.

Gage, K.S. 1990. Radar observations of the free atmosphere: Structure and dynamics. In *Radar in meteorology*, ed. D. Atlas, 534–565. Boston: American Meteorological Society.

Gage, K.S., and B.B. Balsley. 1978. Doppler radar probing of the clear atmosphere. *Bulletin of the American Meteorological Society* 59: 1074–1093.

Gage, K.S, and B.B. Balsley. 1980. On the scattering and reflection mechanisms contributing to clear air radar echoes from the troposphere, stratosphere, and mesosphere. *Radio Science* 15: 243–257.

Gage, K.S., and J.L. Green. 1978. Evidence for specular reflection from monostatic VHF radar observations of the atmosphere. *Radio Science* 13: 991–1001.

Gage, K.S., and J.L. Green. 1979. Tropopause detection by partial specular reflection with very-high-frequency radar. *Science* 203: 1238–1240.

Gage, K.S., and J.L. Green. 1982. An objective method for the determination of tropopause height from VHF radar observations. *Journal of Applied Meteorology* 21: 1150–1154.

Gage, K.S., B.B. Balsley, and J.L. Green. 1981. Fresnel scattering model for the specular echoes observed by VHF radar. *Radio Science* 16: 1447–1453.

Gage, K.S., W.L. Ecklund, and B.B. Balsley. 1985. A modified Fresnel scattering model for the parameterization of Fresnel returns. *Radio Science* 20: 1493–1501.

Gage, K.S., B.B. Balsley, W.L. Ecklund, D.A. Carter, and J.R. McAfee. 1991. Wind profiler-related research in the tropical Pacific. *Journal of Geophysical Research* 96: 3209–3220.

Gage, K.S., J.R. McAfee, and C.R. Williams. 1996. On the annual variation of tropospheric zonal winds observed above Christmas Island in the central equatorial Pacific. *Journal of Geophysical Research* 101: 15061–15070.

Gavrilov, N.M. 1992. Internal gravity waves in the mesopause region: Hydrodynamic sources and climatological patterns. *Advances in Space Research* 12: 10113–10121.

Gavrilov, N.M., S. Fukao, T. Nakamura, T. Tsuda, M.D. Yamanaka, and M. Yamamoto. 1996. Statistical analysis of gravity waves observed with the middle and upper atmosphere radar in the middle atmosphere, 1. Method and general characteristics. *Journal of Geophysical Research* 101: 29511–29521.

Gavrilov, N.M., S. Fukao, and H. Hashiguchi. 1999. Multi-beam MU radar measurements of advective accelerations in the atmosphere. *Geophysical Research Letters* 26: 315–318.

Geerts, B., and P.V. Hobbs. 1991. Organization and structure of clouds and precipitation on the Mid-Atlantic Coast of the United States of America. Part IV: Retrieval of the thermodynamic and cloud microphysical structure of a frontal rainband from Doppler radar data. *Journal of the Atmospheric Sciences* 48: 1287–1305.

Geller, M.A. 1983. Dynamics of the middle atmosphere (Tutorial lecture). *Space Science Reviews* 34: 359–375.

Gill, A.E. 1982. *Atmosphere-ocean dynamics*, 662 pp. London: Academic.

Gordon, W.E. 1958. Incoherent scattering of radio waves by free electrons with applications to space explorations by radar. *Proceedings of the IRE* 46: 1824–1829.

Gordon, W.E., and L.M. LaLonde. 1961. The design and capabilities of an ionospheric radar probe. *IRE Transactions on Antennas and Propagation* AP-9: 17–22.

Gorgucci, E., G. Scarchilli, and V. Chandrasekar. 1999. Specific differential phase estimation in the presence of nonuniform rainfall medium along path. *Journal of Atmospheric and Oceanic Technology* 16: 1690–1697.

Gossard, E.E., and R.G. Strauch. 1983. *Radar observation of clear air and clouds*, 280 pp. Amsterdam: Elsevier.

Gossard, E.E., J.H. Richter, and D. Atlas. 1970. Internal waves in the atmosphere from high-resolution radar measurements. *Journal of Geophysical Research* 75: 3523–3536.

Gossard, E.E., S. Gutman, B.B. Stankov, and D.E. Wolfe. 1999. Profile of radio refractive index and humidity derived from radar wind profilers and the Global Positioning System. *Radio Science* 34: 371–383.

Gunn, K.L.S., and T.W.R. East. 1954. The microwave properties of precipitation particles. *Quarterly Journal of the Royal Meteorological Society* 80: 522–545.

Gunn, R., and G.D. Kinzer. 1949. The terminal velocity of fall for water droplets in stagnant air. *Journal of Meteorology* 6: 243–248.

Gunn, K.L.S., and R.S. Marshall. 1958. The distribution of size of aggregate snowflakes. *Journal of Meteorology* 15: 452–466.

Hamazu, K. 2002. *Development of Doppler radars for studying aviation weather*, 207 pp. Ph.D. dissertation. Kyoto University.

Hamazu, K., K. Hata, M. Ishihara, H. Hashiguchi, and S. Fukao. 2000a. Development of a C-band Doppler radar for low-level wind shear detection. *IEICE, J83-B* 6: 894–909 (in Japanese).

Hamazu, K., M. Ishihara, K. Hata, H. Hashiguchi, and S. Fukao. 2000b. Development of a low-level wind shear detection algorithm for a Doppler weather radar. *IEICE, J83-B* 7: 1067–1080 (in Japanese).

Hamazu, K., K. Hemmi, K. Hayashi, H. Hashiguchi, and S. Fukao. 2002. Development of a 5.3-GHz klystron for a pulse Doppler radar. *IEICE* E85-B: 1152–1159.

Hamazu, K., H. Hashiguchi, T. Wakayama, T. Matsuda, R.J. Doviak, and S. Fukao. 2003. A 35-GHz scanning Doppler radar for fog observations. *Journal of Atmospheric and Oceanic Technology* 20: 972–986.

Hanle, E. 1986. Survey of bistatic and multistatic radar. *Proceedings of the IEE* 133: 587–595.

Hansen, R.C. 2009. *Phased array antennas*, 547 pp. 2nd ed. Hoboken: Wiley.

Hardy, K.R., and H. Ottersten. 1969. Radar investigations of convective patterns in the clear atmosphere. *Journal of the Atmospheric Sciences* 26: 666–672.

Harris, F.J. 1978. On the use of windows for harmonic analysis with the discrete Fourier transform. *Proceedings of the IEEE* 66: 51–83.

Hartree, D.R., J.G. Michel, and P. Nicolson. 1946. Practical methods for the solution of the equations of tropospheric refraction. In *Meteorological factors in radio wave propagation*, 127–168. London: Physical Society.

Hashiguchi, H., M. Yamamoto, S. Fukao, T. Tsuda, M.D. Yamanaka, T. Nakamura, T. Sato, S. Kato, T. Makihira, and K. Hamazu. 1992. Development of a boundary layer radar. In *International symposium on middle atmosphere science (preprints)*, 23–37 March, Kyoto, 46–47.

Hashiguchi, H., M.D. Yamanaka, T. Tsuda, M. Yamamoto, T. Nakamura, T. Adachi, S. Fukao, T. Sato, and D.L. Tobing. 1995a. Diurnal variations of the planetary boundary layer observed with an L-band clear-air Doppler radar. *Boundary-Layer Meteorology* 74: 419–424.

Hashiguchi, H., S. Fukao, T. Tsuda, M.D. Yamanaka, D.L. Tobing, T. Sribimawati, S.W.B. Harijono, and H. Wiryosumarto. 1995b. Observations of the planetary layer over equatorial Indonesia with an L-band clear-air Doppler radar: Initial results. *Radio Science* 30: 1043–1054.

Hashiguchi, H., S. Fukao, Y. Moritani, T. Wakayama, and S. Watanabe. 2004. A lower troposphere radar: 1.3-GHz active phased-array type wind profiler with RASS. *Journal of the Meteorological Society of Japan* 82: 915–931.

Hassenpflug, G., P.B. Rao, M. Yamamoto, and S. Fukao. 2003. MU radar spaced antenna observations with varying apertures: Scatterer and antenna contributions to the ground diffraction pattern. *Radio Science* 38: 1043. doi:10.1029/2002RS002751.

Hassenpflug, G., M. Yamamoto, H. Luce, and S. Fukao. 2008. Description and demonstration of the new middle and upper atmosphere radar imaging system: 1-D, 2-D, and 3-D imaging of troposphere and stratosphere. *Radio Science* 43: 2013. doi:10.1029/2006RS003603.

Hauser, D., and P. Amayenc. 1981. A new method for deducing hydrometeor-size distributions and vertical air motions from Doppler radar measurements at vertical incidence. *Journal of Applied Meteorology* 20: 547–555.

Hauser, D., F. Roux, and P. Amayenc. 1988. Comparison of two method for the retrieval of thermodynamic and microphysical variables from Doppler radar measurements: Application to the case of a tropical squall line. *Journal of the Atmospheric Sciences* 45: 1285–1303.

Heisenberg, W. 1948. On the theory of statistical and isotropic turbulence. *Proceedings of the Royal Society A* 195: 402–406.

Heiss, W.H., D.L. McGrew, and D.S. Sirmans. 1990. NEXRAD; Next generation weather radar (WSR-88D). *Microwave Journal* 33: 79–98.

Hélal D., M. Crochet, H. Luce, and E. Spano. 2001. Radar imaging and high-resolution array processing applied to a classical VHF-ST profiler. *Journal of Atmospheric and Solar-Terrestrial Physics* 63: 263–274.

Herman, B.M., and L.J. Battan. 1961. Calculations of mie back-scattering from melting ice spheres. *Journal of Meteorology* 18: 468–478.

Hill, R.J. 1978. Spectra of fluctuations in refractivity, temperature, humidity, and the temperature–humidity cospectrum in the inertial and dissipation range. *Radio Science* 13: 935–961.

Hill, R.J., and S.F. Clifford. 1978. Modified spectrum of atmospheric temperature fluctuations and its application to optical propagation. *Journal of the Optical Society of America* 68: 892–899.

Hines, C.O. 1968. A possible source of waves in noctilucent clouds. *Journal of the Atmospheric Sciences* 25: 937–942.

Hirono, M., H. Luce, M. Yamamoto, and S. Fukao. 2004. Horizontal maps of echo power in the lower stratosphere using the MU radar. *Annales Geophysicae* 22: 717–724.

Hirota, I., and T. Niki. 1986. Inertia-gravity waves in the troposphere and stratosphere observed by the MU radar. *Journal of the Meteorological Society of Japan* 64: 995–999.

Hitschfeld, W.F., and J. Bordan. 1954. Errors inherent in the radar measurement of rainfall at attenuating wavelengths. *Journal of Meteorology* 11: 58–67.

Hobbs, P.V. 1978. Organization and structure of clouds and precipitation on the mesoscale and microscale in cyclonic storms. *Reviews of Geophysics and Space Physics* 16: 741–755.

Hocking, W.K. 1983. On the extraction of atmospheric turbulence parameters from radar backscatter Doppler spectra—I. Theory. *Journal of Atmospheric and Terrestrial Physics* 45: 89–102.

Hocking, W.K. 1985. Measurement of turbulent energy dissipation rates in the middle atmosphere by radar techniques. A review. *Radio Science* 20: 1403–1422.

Hocking, W.K. 1988. Two years of continuous measurements of turbulence parameters in the upper mesosphere and lower thermosphere made with a 2-MHz radar. *Journal of Geophysical Research* 93: 2475–2491.

Hocking, W.K. 1997a. System design, signal processing procedures and preliminary results for the Canadian (London, Ontario) VHF atmospheric radar. *Radio Science* 32: 687–706.

Hocking, W.K. 1997b. Recent advances in radar instrumentation and techniques for studies of the mesosphere, stratosphere, and troposphere. *Radio Science* 32: 2241–2270.

Hocking, W.K., T. Thayaparan, and J. Jones. 1997. Meteor decay times and their use in determining a diagnostic mesospheric temperature–pressure parameter: Methodology and one year of data. *Geophysical Research Letters* 24: 2977–2980.

Holloway, C.L., R.J. Doviak, and S.A. Cohen. 1997a. Cross correlations of fields scattered by horizontally anisotropic refractive index irregularities. *Radio Science* 32: 1911–1920.

Holloway, C.L., R.J. Doviak, S.A. Cohn, R.J. Lataitis, and J.S. Van Baelen. 1997b. Cross correlations and cross spectra for spaced antenna wind profilers 2. Algorithms to estimate wind and turbulence. *Radio Science* 32: 967–982.

Houze, R.A. Jr. 1993. *Cloud dynamics*, 570 pp. San Diego: Academic.

Houze, R.A. Jr., J.D. Locatelli, and P.V. Hobbs. 1976. Dynamics and cloud microphysics of the rainbands in an occluded frontal system. *Journal of the Atmospheric Sciences* 33: 1921–1936.

Houze, R.A. Jr., S.A. Rutledge, M.I. Biggerstaff, and B.F. Smull. 1989. Interpretation of Doppler weather-radar displays in midlatitude mesoscale convective systems. *Bulletin of the American Meteorological Society* 70: 608–619.

Houze R.A. Jr., B.F. Smull, and P. Dodge. 1990. Mesoscale organization of springtime rainstorms in Oklahoma. *Monthly Weather Review* 117: 613–654.

Hubbert, J., and V.N. Bringi. 1995. An iterative filtering technique for the analysis of copolar differential phase and dual-frequency radar measurements. *Journal of Atmospheric and Oceanic Technology* 12: 643–648.

Hubbert, J., V. Chandrasekar, and V.N. Bringi. 1993. Processing and interpretation of coherent dual-polarized radar measurements. *Journal of Atmospheric and Oceanic Technology* 10: 155–164.

Hubbert, J.C., V.N. Bringi, and D. Brunkow. 2003. Studies of the polarimetric covariance matrix. Part I: Calibration methodology. *Journal of Atmospheric and Oceanic Technology* 20: 696–706.

Hubbert, J.C., S.M. Ellis, M. Dixon, and G. Meymaris. 2010. Modeling, error analysis, and evaluation of dual-polarization variables obtained from simultaneous horizontal and vertical polarization transmit radar, Part II: Experimental data. *Journal of Atmospheric and Oceanic Technology* 27: 1599–1607.

Ice, R.L., R.D. Rhoton, D.S. Saxion, N.K. Patel, D. Sirmans, D.A. Warde, D.L. Rachel, and R.G. Fehlen. 2004. Radar Operations Center (ROC) evaluation of the WSR-88D open radar data acquisition (ORDA) system signal processing. In *20th International conference on interactive information and processing systems for meteorology, oceanography, and hydrology*, Seattle, WA. Boston: American Meteorological Society, paper 5.5.

Ice, R.L., G.T. McGehee, R.D. Rhoton, D.S. Saxion, D.A. Warde, R.G. Guenther, D. Sirmans, and D.L. Rachel. 2005. Radar Operations Center (ROC) evaluation of new signal processing techniques for the WSR-88D. In *21th international conference on interactive information and processing systems for meteorology, oceanography, and hydrology*, San Diego, CA. Boston: American Meteorological Society, paper P1.4.

IEICE. 2008. *Antenna engineering handbook*, 1098 pp. 2nd ed. Tokyo: Ohmsha (in Japanese).

Ishihara, M., Z. Yanagisawa, H. Sakakibara, K. Matsuura and J. Aoyagi. 1986. Structure of a typhoon rainband observed by two Doppler radars. *Journal of the Meteorological Society of Japan* 64: 923–939.

Ishihara, M., Y. Kato, T. Abo, K. Kobayashi, and Y. Izumikawa. 2006. Characteristics and performance of the operational wind profiler network of the Japan Meteorological Agency. *Journal of the Meteorological Society of Japan* 84: 1085–1096.

ITU-R. 2001. Attenuation by atmospheric gases. In *ITU-R Recommendations* ITU-R P. 676-5. Geneva, Switzerland: International Telecommunications Union.

Iwanami, K., R. Misumi, M. Maki, T. Wakayama, K. Hata, and S. Watanabe. 2001. Development of a multiparameter radar system on mobile platform. In *30th Conference on radar meteorology (preprints)*, 104–106. Boston: American Meteorological Society.

Jackson, M.C. 1986. The geometry of bistatic radar systems. *Proceedings of the IEE* 133: 604–612.

Jameson, A.R. 1985. Microphysical interpretation of multiparameter radar measurements in rain, Part III: Interpretation and measurement of propagation differential phase shift between orthogonal linear polarizations. *Journal of the Atmospheric Sciences* 42: 607–614.

Jameson, A.R. 1992. The effect of temperature on attenuation correction schemes in rain using polarization propagation differential phase shift. *Journal of Applied Meteorology* 31: 1106–1118.

Jameson, A.R., and D.B. Johnson. 1990. Cloud microphysics and radar. In *Radar in meteorology*, ed. D. Atlas, 323–340. Boston: American Meteorological Society.

Janssen, L., and G. van der Spek. 1985. The shape of Doppler spectra from precipitation. *IEEE Trans. Aerosp. Electron. Syst.* 21: 208–219.

Johnson, R.H., and P.J. Hamilton. 1988. The relationship of surface pressure features to the precipitation and airflow structure of an intense midlatitude squall line. *Monthly Weather Review* 116: 1444–1472.

Jorgensen, D.P., and P.T. Willis. 1982. A Z-R relationship for hurricanes. *Journal of Applied Meteorology* 21: 356–366.

Joss, J., and A. Waldvogel. 1970. A method to improve the accuracy of radar-measured amounts of precipitation. In *14th Conference on radar meteorology (preprints)*, 237–238. Boston: American Meteorological Society.

Kato, S. 1980. *Dynamics of the upper atmosphere*, 233 pp. Dordrecht: D. Reidel Publishing.

Kato, S., K. Fukuyama, K. Wakasugi, T. Sato, and S. Fukao. 1982. Middle atmosphere observations with large scale MST radar. Research Note. *Journal of the Meteorological Society of Japan* **144**, 1–55 (in Japanese).

Kato, S., T. Ogawa, T. Tsuda, T. Sato, I. Kimura, and S. Fukao. 1984. The middle and upper atmosphere radar: First results using a partial system. *Radio Science* 19: 1475–1484.

Kawashima, M., K. Tsuboki, and T. Asai. 1995. Maintenance mechanism and thermodynamic structure of a Baiu frontal rainband retrieved from dual Doppler radar observations. *Journal of the Meteorological Society of Japan* 73: 717–735.

Keenan, T.D. 2003. Hydrometeor classification with a C-band polarimetric radar. *Australian Meteorological Magazine* 52: 23–31.

Keer, D.E. 1951. *Propagation of short radio waves*, 728 pp. New York: McGraw-Hill.

Kilburn, C., S. Fukao, and M. Yamamoto. 1995. Extended period frequency domain interferometry observations at stratospheric and tropospheric heights. *Radio Science* 30: 1099–1109.

Kingsmill, D.E., and R.M. Wakimoto. 1991. Kinematic, dynamic, and thermodynamic analysis of a weakly sheared thunderstorm over northern Alabama. *Monthly Weather Review* 119: 262–297.

Kobayashi, T., and A. Adachi. 2001. Measurements of rain-drop breakup by using UHF wind profilers. *Geophysical Research Letters* 28: 4071–4072.

Kodaira, N. 1990. History of radar meteorology in Japan. In *Radar in meteorology*, ed. D. Atlas, 69–76. Boston: American Meteorological Society.

Komabayashi, M., T. Gonda, and K. Isono. 1964. Lifetime of water drops before breaking and size distribution of fragment drops. *Journal of the Meteorological Society of Japan* 42: 330–340.

Konrad, T.G. 1970. The dynamics of the convective process in clear air as seen by radar. *Journal of the Atmospheric Sciences* 27: 1138–1147.

Koscielny, A.J., R.J. Doviak, and R. Rabin. 1982. Statistical considerations in the estimation of divergence from single-Doppler radar and application to prestorm boundary-layer observations. *Journal of Applied Meteorology* 21: 197–210.

Kozu, T., T. Kawanishi, H. Kuroiwa, M. Kojima, K. Oikawa, H. Kumagai, K. Okamoto, M. Okumura, H. Nakatsuka, and K. Nishikawa. 2001. Development of precipitation radar onboard the Tropical Rainfall Measuring Mission (TRMM) satellite. *IEEE Transactions on Geoscience and Remote Sensing* 39: 102–116.

Kozu, T., T. Shimomai, Z. Akramin, Marzuki, Y. Shibagaki, and H. Hashiguchi. 2005. Intraseasonal variation of raindrop size distribution at Koto Tabang, West Sumatra, Indonesia. *Geophysical Research Letters* 32: L07803. doi:10.1029/2004GL022340.

Kropfli, R.A., S.Y. Matrosov, T. Uttal, B.W. Orr, A.S. Frisch, K.A. Clark, B.W. Bartram, R.F. Reinking, J.B. Snider, and B.E. Martner. 1995. Cloud physics studies with 8 mm wavelength radar. *Atmospheric Research* 35: 299–313.

Kudeki, E., and G.R. Stitt. 1987. Frequency domain interferometry: A high resolution radar technique for studies of atmospheric turbulence. *Geophysical Research Letters* 14: 198–201.

Kudeki, E., and F. Sürücü. 1991. Radar interferometric imaging of field-aligned plasma irregularities in the equatorial electrojet. *Geophysical Research Letters* 18: 41–44.

Kudeki, E., and R.F. Woodman. 1990. A post-statistic steering technique for MST radar applications. *Radio Science* 25: 591–594.

Kurosaki, S., M.D. Yamanaka, H. Hashiguchi, T. Sato, and S. Fukao. 1996. Vertical eddy diffusivity in the lower and middle atmosphere: A climatology based on the MU radar observations during 1986–1992. *Journal of Atmospheric and Terrestrial Physics* 58: 727–734.

Laird, B.G. 1981. On ambiguity resolution by random phase processing. In *20th International conference on radar meteorology (preprints)*, 327–331. Boston: American Meteorological Society.

Laird, B.G., and J.E. Evans. 1982. FAA weather radar surveillance requirements in the context of NEXRAD. *MIT Lincoln Laboratory Project Rep.*, ATC-112, DOT/FAA-RD-81-111.

Lane, J.A., and J.A. Saxton. 1952. Dielectric dispersion in pure polar liquids at very high radio frequencies. *Proceedings of the Royal Society A* 213: 400–408.

Larsen, M.F., R.D. Palmer, S. Fukao, R.F. Woodman, M. Yamamoto, T. Tsuda, and S. Kato. 1992. An analysis technique for deriving vector winds and in-beam incidence angles from radar interferometer measurements. *Journal of Atmospheric and Oceanic Technology* 9: 3–14.

Law, D.C., K.P. Moran, R.G. Frehlich, and R.G. Strauch. 1994. Maximum likelihood estimation of spectral moments in the presence of clutter. In *Extended abstracts of the third international symposium on tropospheric profiling: needs and technologies*, August 30–September 2, Hamburg, Germany, 216–218.

Le, K.D., R.D. Palmer, B.L. Cheong, T.-Y. Yu, G. Zhang, and S.M. Torres. 2010. Reducing the effects of noise on atmospheric imaging radars using multilag correlation. *Radio Science* 45: 1008. doi:10.1029/2008RS003989.

Leary, C.A., and R.A. Houze, Jr. 1979. The structure and evolution of convection in a tropical cloud cluster. *Journal of the Atmospheric Sciences* 36: 437–457.

Lhermitte, R.M. 1968. Turbulent air motion as observed by Doppler radar. In *13th Conference on radar meteorology (preprints)*, 498–503. Boston: American Meteorological Society.

Lhermitte, R.M. 1970. Dual-Doppler radar observations of convective storm circulation. In *14th Conference on radar meteorology (preprints)*, 139–144. Boston: American Meteorological Society.

Lhermitte, R.M., and L.J. Miller. 1970. Doppler radar methodology for the observation of convective storms. In *14th Conference on radar meteorology (preprints)*, 133–138. Boston: American Meteorological Society.

Liebe, H.J. 1985. An updated model for millimeter wave propagation in moist air. *Radio Science* 20: 1069–1089.

Lilly, D.K., D.E. Waco, and S.I. Adelfang. 1974. Stratospheric mixing estimated from high-latitude turbulence measurements. *Journal of Applied Meteorology* 13: 488–493.

Lindzen, R.S. 1984. Gravity waves in the mesosphere. In *Dynamics of the middle atmosphere*, 3–18. Tokyo: Dordrecht Press.

Liu, H., and V. Chandrasekar. 2000. Classification of hydrometeors based on polarimetric radar measurements: Development of fuzzy logic and neuro-fuzzy systems, and in situ verification. *Journal of Atmospheric and Oceanic Technology* 17: 140–164.

Liu, C.H., J. Röttger, G. Dester, S.J. Franke, and C.-J. Pan. 1991. The oblique spaced antenna method for measuring the atmospheric wind field. *Journal of Atmospheric and Oceanic Technology* 8: 247–258.

Liu, S., Q. Xu, and P. Zhang. 2005. Identifying Doppler velocity contamination caused by mitigating birds, Part II: Bays identification and probability tests. *Journal of Atmospheric and Oceanic Technology* 22: 1114–1121.

Lopez-Dekker, P.L., and S.J. Frasier. 2004. Radio acoustic sounding with a UHF volume imaging radar. *Journal of Atmospheric and Oceanic Technology* 21: 766–776.

Lott, F., and H. Teitelbaum. 1993. Topographic waves generated by a transient wind. *Journal of the Atmospheric Sciences* 50: 2607–2654.

Luce, H., M. Crochet, F. Dalaudier, and C. Sidi. 1995. Interpretation of VHF ST radar vertical echoes from in-situ temperature sheet observations. *Radio Science* 30: 1002–1025.

Luce, H., S. Fukao, and M. Yamamoto. 2001a. Validation of winds measured by MU radar with GPS radiosondes during the MUTSI campaign. *Journal of Atmospheric and Oceanic Technology* 18: 817–829.

Luce, H., M. Yamamoto, S. Fukao, and M. Crochet. 2001b. Extended radar observations with the frequency radar domain interferometric imaging (FII) technique. *Journal of Atmospheric and Solar-Terrestrial Physics* 63: 221–234.

Luce, H., S. Fukao, F. Dalaudier, and M. Crochet. 2002. Strong mixing events observed near the tropopause with the MU radar and high-resolution balloon techniques. *Journal of the Atmospheric Sciences* 59: 2885–2896.

Luce, H., G. Hassenpflug, M. Yamamoto, and S. Fukao. 2007. Comparisons of refractive index gradient and stability profiles measured by balloons and the MU radar at a high vertical resolution in the lower stratosphere. *Annales Geophysicae* 25: 47–57.

Luce, H., G. Hassenpflug, M. Yamamoto, S. Fukao, and K. Sato. 2008. High-resolution observations with MU radar of a KH instability triggered by an inertia-gravity wave in the upper part of a jet-stream. *Journal of the Atmospheric Sciences* 65: 1711–1718.

Lyons, R.G. 2004. *Understanding Digital Signal Processing*, 665 pp. 2nd ed. Boston: Prentice Hall.

Maeda, K., H. Alvarez, J. Aparici, J. May, and P. Reich. 1999. A 45-MHz continuum survey of the northern hemisphere. *Astronomy and Astrophysics Supplement Series* 140: 145–154.

Maekawa, Y., S. Fukao, T. Sato, S. Kato, and R.F. Woodman. 1984. Internal inertia-gravity waves in the tropical lower stratosphere observed by the Arecibo radar. *Journal of the Atmospheric Sciences* 41: 2359–2367.

Maguire, W.B., and S.K. Avery. 1995. Retrieval of raindrop size distributions using two Doppler wind profilers: model sensitivity testing. *Journal of Applied Meteorology* 33: 1623–1635.

Mahapatra, P.R. 1999. *Aviation weather surveillance systems*, 453 pp. Reston: AIAA.

Maki, M., S.G. Park, and V.N. Bringi. 2005. Effect of natural variations in rain drop size distributions on rain rate estimation of 3 cm wavelength polarimetric radar. *Journal of the Meteorological Society of Japan* 83: 871–893.

Manzini, E., and K. Hamilton. 1993. Middle atmospheric travelling waves forced by latent and convective heating. *Journal of the Atmospheric Sciences* 50: 2180–2200.

Marcuvitz, N. 1965. *Waveguide handbook*, 428 pp. New York: Dover Publications.

Marks, F.D., Jr., and R.A. Houze, Jr. 1987. Inner-core structure of Hurricane Alicia from airborne Doppler-radar observations. *Journal of the Atmospheric Sciences* 44: 1296–1317.

Marshall, J.S., and W.M. Palmer. 1948. The distribution of raindrops with size. *Journal of Meteorology* 5: 165–166.

Marshall, J.S., W. Hitschfeld, and K.L.S. Gunn. 1955. Advances in radar weather. *Advances in Geophysics* 2: 1–56.

Marshall, J.M., A.M. Peterson, and A.A. Barnes, Jr. 1972. Combined radar-acoustic sounding system. *Applied Optics* 11: 108–112.

Masuda, Y. 1988. Influence of wind and temperature on the height limit of a radio acoustic sounding system. *Radio Science* 23: 647–654.

Masuda, Y., J. Awaka, K. Nakamura, T. Adachi, and T. Tsuda. 1992. Analysis of the radio sounding system using a chirped acoustic wave. *Radio Science* 27: 681–691.

Matrosov, S.Y., K.A. Clark, and B.E. Martner. 2002. X-band polarimetric radar measurements of rainfall. *Journal of Applied Meteorology* 41: 941–952.

Matson, R.J., and A.W. Huggins. 1980. The direct measurement of the size, shapes and kinematics of falling hailstones. *Journal of the Atmospheric Sciences* 37: 1107–1125.

Matuura, N., Y. Masuda, H. Inuki, S. Kato, S. Fukao, T. Sato, and T. Tsuda. 1986. Radio acoustic measurement of temperature profile in the troposphere and stratosphere. *Nature* 323: 426–428.

May, P.T., and T.D. Keenan. 2005. Evaluation of microphysical retrievals from polarimetric radar with wind profiler data. *Journal of Applied Meteorology* 44: 827–838.

May, P.T., S. Fukao, P.J. Neiman, M.W. Kozleski, M.D. Yamanaka, S. Kato, M. Yamamoto, T. Sato, and T. Tsuda. 1992. MU radar observations of the wind field in the vicinity of the Baiu front during early July, 1987. *Beitraege zur Physik der Atmosphaere (Contributions To Atmospheric Physics)* 65: 3–11.

May, P.T., G.T. Holland, and W.L. Ecklund. 1994. Wind profiler observation of tropical storm Flo at Saipan. *Weather and Forecasting* 9: 410–426.

McCarthy, J., and J.W. Wilson. 1985. The Classify, Locate, and Avoid Wind Shear (CLAWS) project at Denver's Stapleton International Airport: Operational testing of terminal weather hazard warnings with an emphasis on microburst wind shear. In *Second international conference on the aviation weather system*, Montreal, 247–256. Boston: American Meteorological Society.

McCarthy, J., W. Frost, B. Terkel, R.J. Doviak, D.W. Camp, E.F. Blick, and K.L. Elmore. 1980. An airport wind shear detection and warning system using Doppler radar. In *19th Conference on radar meteorology (preprints)*, Miami, FL, 135–142. Boston: American Meteorological Society.

McKinley, D.W.R. 1961. *Meteo science and engineering*, 309 pp. New York: McGraw-Hill.

Mead, J.B., G. Hopcraft, S.J. Frasier, B.D. Pollard, C.D. Cherry, D.H. Schaubert, and R.E. McIntoch. 1998. A volume-imaging radar wind profiler for atmospheric boundary layer turbulence studies. *Journal of Atmospheric and Oceanic Technology* 15: 849–859.

Melnikov, V.M. 2006. One-lag estimators for cross-polarization measurements. *Journal of Atmospheric and Oceanic Technology* 23: 915–926.

Melnikov, V.M., R.J. Doviak, D.S. Zrnić, and D.J. Stensrud. 2011. Mapping Bragg scatter with a polarimetric WSR-88D. *Journal of Atmospheric and Oceanic Technology* 28: 1273–1285.

Meymaris, G. 2007. The use of spectral processing to improve radar spectral moment. In *23rd Conference on interactive information and processing systems for meteorology, oceanography, and hydrology (preprints)*, San Antonio, TX. Boston: American Meteorological Society, 8A.4.

Michelson, M., W.W. Shrader, and J.G. Wieler. 1990. Terminal Doppler weather radar. *Microwave Journal* 33: 139–148.

Miyashita, H., H. Ohmine, K. Nishizawa, S. Makino, and S. Urasaki. 1999. Electromagnetically coupled coaxial dipole array antenna. *IEEE Transactions on Antennas and Propagation* 47: 1716–1726.

Moran, K.P., E.B. Martner, M.J. Post, R.A. Kropfli, D.C. Welsh, and K.B. Widener. 1998. An unattended cloud-profiling radar for use in climate research. *Bulletin of the American Meteorological Society* 79: 443–455.

Mori, S., J.-I. Hamada, M.D. Yamanaka, Y.-M. Kodama, M. Kawashima, T. Shimomai, Y. Shibagaki, H. Hashiguchi and T. Sribimawati. 2006. Vertical wind characteristics in precipitating cloud systems over West Sumatera, Indonesia, observed with Equatorial Atmosphere Radar: Case Study of 23–24 April 2004 during the first CPEA campaign period. *Journal of the Meteorological Society of Japan* 84: 113–131.

Muraoka, Y., K. Kawahira, T. Sato, T. Tsuda, S. Fukao, and S. Kato. 1987. Characteristics of inertial gravity waves in the mesosphere observed by the MU radar. *Geophysical Research Letters* 14: 1154–1157.

Murayama, Y., T. Tsuda, and S. Kato. 1994. Seasonal variation of gravity wave activity in the lower atmosphere observed with the MU radar. *Journal of Geophysical Research* 99: 23057–23069.

Muschinski, A., and C. Wode. 1998. First in situ evidence for coexisting submeter temperature and humidity sheets in the lower free troposphere. *Journal of the Atmospheric Sciences* 55: 2893–2906.

Nakamura, K., and Y. Masuda. 1992. Development of a lower troposphere wind profiler at Communications Research Laboratory. In *International symposium on middle atmosphere science (preprints)*, Kyoto, 23–37 March, 48–49.

Nastrom, G.D., and D.C. Fritts. 1992. Sources of mesoscale variability of gravity waves, Part 1: Topographic excitation. *Journal of the Atmospheric Sciences* 49: 101–110.

Nathanson, F.E. 1991. *Radar design principles*, 720 pp. 2nd ed. Mendham: SciTech.

Nathanson, F.E., and J.P. Reilly. 1968. Radar precipitation echoes. *IEEE Transactions on Aerospace and Electronic Systems* AES-4: 505–514.

Nathanson, F.E., and P.L. Smith. 1972. A modified coefficient for the weather radar equation. In *15th Conference radar meteorology (preprints)*, 228–230. Boston: American Meteorological Society.

Nelson, S.P., and R.A. Brown. 1987. Error sources and accuracy of vertical velocities computed from multiple-Doppler radar measurements in deep convective storms. *Journal of Atmospheric and Oceanic Technology* 4: 234–238.

Nickel, U. 1988. Algebraic formulation of Kumaresan-Tuffs superresolution method, showing relation to ME and MUSIC method. *IEE Proceedings* 135: 7–10.

Nishi, N., M.K. Yamamoto, T. Shimomai, A. Hamada, and S. Fukao. 2007. Fine structure of vertical motion in the stratiform precipitation region observed by a VHF Doppler radar installed in Sumatra, Indonesia. *Journal of Applied Meteorology and Climatology* 46: 522–537.

Ochs, G.R. 1965. The large 50 Mc/s dipole array at Jicamarca Radar Observatory. *NBS Rep.,* 8772, 61 pp. National Bureau of Standards, Boulder, CO.

Ogawa, T., and T. Shimazaki. 1975. Diurnal variations of odd nitrogen and ionic densities in the mesosphere and lower thermosphere: Simultaneous solution of photochemical-diffusive equations. *Journal of Geophysical Research* 80: 3945–3960.

Oguchi, T. 1983. Electromagnetic wave propagation and scattering in rain and other hydrometeors. *Proceedings of the IEEE* 71: 1029–1078.

Ogura, H. 1998. *Introduction to stochastic process*, 212 pp. Tokyo: Morikita-Suppan (in Japanese).

Ogura, Y., and N.A. Phillips. 1962. Scale analysis of deep and shallow convection in the atmosphere. *Journal of the Atmospheric Sciences* 19: 1458–1476.

Ogura, H., and Y. Yoshida. 1981. Spectral analysis and subtraction of noise in radar signals. *IEEE Transactions on Aerospace and Electronic Systems* AES-17: 62–71.

Orlansky, I. 1975. A rational subdivision of scales for atmospheric processes. *Bulletin of the American Meteorological Society* 56: 527–530.

O'Sullivan, D., and T.J. Dunkerton. 1995. Generation of inertia-gravity waves in a simulated life cycle of baroclinic instability. *Journal of the Atmospheric Sciences* 52: 3695–3716.

Ottersten, H. 1969a. Atmospheric structure and radar backscattering in clear air. *Radio Science* 4: 1179–1193.

Ottersten, H. 1969b. Radar backscattering from the turbulent clear atmosphere. *Radio Science* 4: 1251–1255.

Ottersten, H. 1969c. Mean vertical gradient of potential refractive index in turbulent mixing and radar detection of CAT. *Radio Science* 4: 1247–1249.

Palmer, R.D., R.F. Woodman, S. Fukao, T. Tsuda, and S. Kato. 1990. Three-antenna poststatistic steering using the MU radar. *Radio Science* 25: 1105–1110.

Palmer, R.D., S. Fukao, M.F. Larsen, R.F. Woodman, M. Yamamoto, T. Tsuda, and S. Kato. 1991. VHF radar interferometry measurements of vertical velocity and the effects of tilted refractivity surfaces on standard Doppler measurements. *Radio Science* 26: 417–427.

Palmer, R.D., M.F. Larsen, E.L. Sheppard, S. Fukao, M. Yamamoto, T. Tsuda, and S. Kato. 1993. Poststatistic steering wind estimation in the troposphere and lower stratosphere. *Radio Science* 28: 261–271.

Palmer, R.D., S. Gopalam, T.Y. Yu, and S. Fukao. 1998. Coherent radar imaging using the Capon's method. *Radio Science* 33: 1585–1598.

Palmer, R.D., T.Y. Yu, and P.B. Chilson. 1999. Range imaging using frequency diversity. *Radio Science* 34: 1485–1496.

Palmer, R.D., B.L. Cheong, M.W. Hoffman, S.J. Frasier, and F.J. López-Dekker. 2005. Observations of the small-scale variability of precipitation using an imaging radar. *Journal of Atmospheric and Oceanic Technology* 22: 1122–1137.

Papoulis, A. 1991. *Provability, random variables, and stochastic processes*, 666 pp. 3rd ed. Boston: WCB/McGraw-Hill.

Park, S.-G., V.N. Bringi, V. Chandrasekar, M. Maki, and K. Iwanami. 2005a. Correction of radar reflectivity and differential reflectivity for rain attenuation at X band, Part I: Technical and empirical basis. *Journal of Atmospheric and Oceanic Technology* 22: 1621–1632.

Park, S.-G., M. Maki, K. Iwanami, V.N. Bringi, and V. Chandrasekar. 2005b. Correction of radar reflectivity and differential reflectivity for rain attenuation at X band, Part II: Evaluation and application. *Journal of Atmospheric and Oceanic Technology* 22: 1633–1655.

Park, H., A.V. Ryzhkov, D.S. Zrnić, and K.E. Kim. 2009. The hydrometeor classification algorithm for the polarimetric WSR-88D: Description and application to an MCS. *Weather and Forecasting* 24: 730–748.

Pasqualucci, F. 1984. Drop size distribution measurements in convective storms with a vertically pointing 35-GHz Doppler radar. *Radio Science* 19: 177–183.

Pekour, M.S., and R.L. Coulter. 1999. A technique for removing the effect of migrating birds in 915-MHz wind profiler data. *Journal of Atmospheric and Oceanic Technology* 16: 1941–1948.

Pfeifer, M., G. C. Craig, M. Hagen, and C. Keil. 2008. A polarimetric radar forward operator for model evaluation. *Journal of Applied Meteorology and Climatology* 47: 3202–3220.

Pfister, L., K.R. Chan, T.P. Bui, S. Bowen, M. Legg, B. Gary, K. Kelly, M. Proffitt, and W. Starr. 1993. Gravity waves generated by a tropical cyclone during the STEP tropical field program: A case study. *Journal of Geophysical Research* 98: 8611–8638.

Prichard, I.T., L. Thomas, and R.M. Worthington. 1995. The characteristics of mountain waves observed by radar near the west coast of Wales. *Annales Geophysicae* 13: 757–767.

Probert-Jones, J.R. 1962. The radar equation in meteorology. *Quarterly Journal of the Royal Meteorological Society* 88: 485–495.

Protat, A., and I. Zawadzki. 1999. A variational method for real-time retrieval of three-dimensional wind multiple-Doppler bistatic radar network data. *Journal of Atmospheric and Oceanic Technology* 16: 432–449.

Pruppacher, H.R., and K.V. Beard. 1970. A wind tunnel investigation of the internal circulation and shape of water drops falling at terminal velocity in air. *Quarterly Journal of the Royal Meteorological Society* 96: 247–256.

Ramo, S., J.R. Whinnery, and T. Van Duzer. 1965. *Fields and waves in communication electronics*, 265 pp. New York: Wiley.

Rao, P.B., A.R. Jain, P. Kishore, P. Balamuralidhar, S.H. Damle, and G. Viswanathan. 1995. Indian MST radar, 1. System description and sample vector wind measurements in ST mode. *Radio Science* 30: 1125–1138.

Rao, Q., H. Hashiguchi, and S. Fukao. 2003. Study on ground clutter prevention fences for boundary layer radars. *Radio Science* 38: 1030. doi:10.1029/2001RS002489.

Ratcliffe, J.A. 1956. Some aspects of diffraction theory and their application to the ionosphere. *Reports on Progress in Physics* 19: 188–267.

Ray, P.S., R.J. Doviak, G.B. Walker, D. Sirmans, J. Carter, and B. Bumgarner. 1975. Dual-Doppler observation of tornadic storm. *Journal of Applied Meteorology* 17: 1201–1212.

Ray, P.S., C.L. Zeigler, R.J. Serafin, and W. Bumgarner. 1980. Single- and multiple-Doppler radar observations of tornadic storms. *Monthly Weather Review* 108: 1607–1625.

Reid, I.M., and R.A. Vincent. 1987. Measurements of mesospheric gravity wave momentum fluxes and mean flow acceleration at Adelaide, Australia. *Journal of Atmospheric and Terrestrial Physics* 49: 443–460.

Renggono, F., H. Hashiguchi, S. Fukao, M.D. Yamanaka, S.-Y. Ogino, N. Okamoto, F. Murata, B.P. Sitorus, M. Kudsy, M. Kartasasmita, and G. Ibrahim. 2001. Precipitating clouds observed by 1.3-GHz boundary layer radars in equatorial Indonesia. *Annales Geophysicae* 19: 889–897.

Renggono, F., M.K. Yamamoto, H. Hashiguchi, S. Fukao, T. Shimomai, M. Kawashima, and M. Kudsy. 2006. Raindrop size distribution observed with the Equatorial Atmosphere Radar (EAR) during the CPEA-I observation campaign. *Radio Science* 41: RS5002. doi:10.1029/2005RS003333.

Rodi, A.R., K.L. Elmore, and W.P. Mahoney. 1983. Aircraft and Doppler air motion comparisons in a JAWS microburst. *21st Conference on Radar Meteorology (preprints)*, Edmonton, 624–629. Boston: American Meteorological Society.

Röttger, J. 1979. VHF radar observations of a frontal passage. *Journal of Applied Meteorology* 18: 85–91.

Röttger, J. 1980a. Reflection and scattering of VHF radar signals from atmospheric refractivity structures. *Radio Science* 15: 259–276.

Röttger, J. 1980b. Structure and dynamics of the stratosphere and mesosphere revealed by VHF radar investigations. *Pure and Applied Geophysics* 118: 494–527.

Röttger, J. 1981. Investigations of lower and middle atmosphere dynamics with spaced antenna drifts radars. *Journal of Atmospheric and Terrestrial Physics* 43: 277–292.

Röttger, J., and H.M. Ierkic. 1985. Postbeam steering and interferometry applications of VHF radars to study winds, waves, and turbulence in the lower and middle atmosphere. *Radio Science* 20: 1461–1480.

Röttger, J., and M.F. Larsen. 1990. UHF/VHF radar techniques for atmospheric research and wind profiler applications.In *Radar in meteorology*, ed. D. Atlas, 235–281. Boston: American Meteorological Society.

Röttger, J., and C.H. Liu. 1978. Partial reflection and scattering of VHF radar signals from the clear atmosphere. *Geophysical Research Letters* 5: 357–360.

Röttger, J., and R.A. Vincent. 1978. VHF radar studies of tropospheric velocities and irregularities using spaced antenna techniques. *Geophysical Research Letters* 5: 917–920.

Röttger, J., J. Klostermeyer, P. Czechowsky, R. Rüster, and G. Schmidt. 1978. Remote sensing of the atmosphere by VHF radar experiment. *Naturwissenschaften* 65: 285–296.

Röttger, J., C.-H. Liu, J.K. Chao, A.J. Chen, Y.H. Chu, I.-J. Fu, C.M. Huang, Y.W. Kiang, F.S. Kuo, and C.J. Pan. 1990a. The Chung-Li VHF radar: Technical layout and a summary of initial results. *Radio Science* 25: 478–502.

Röttger, J., C.-H. Liu, C.J. Pan, and I.-J. Fu. 1990b. Spatial interferometry measurements with the Chung-Li VHF radar. *Radio Science* 25: 503–515.

Ryde, J.W. 1946. The attenuation and radar echoes produced at centimetre wavelengths by various meteorological phenomena. In *Meteorological factors in radio wave propagation*, 169–188. London: Physical Society.

Ryzhkov, A.V., and D.S. Zrnić. 1998. Polarimetric rainfall estimation in the presence of anomalous propagation. *Journal of Atmospheric and Oceanic Technology* 15: 1320–1330.

Ryzhkov, A.V., S.E. Giangrande, and T.J. Schuur. 2005. Rainfall estimation with a polarimetric prototype of WSR-88D. *Journal of Applied Meteorology* 44: 502–515.

Saad, Y. 2003. *Iterative methods for space linear systems*, 528 pp. Philadelphia: Siam.

Sachindananda, M., and D.S. Zrnić. 1985. Z_{DR} measurement considerations for a fast scan capability radar. *Radio Science* 20: 907–922.

Sachidananda, M., and D.S. Zrnić. 1986. Recovery of spectral moments from overlaid echoes in a Doppler weather radar. *IEEE Transactions on Geoscience and Remote Sensing* 24: 751–764.

Sachidananda, M., and D.S. Zrnić. 1999. Systematic phase codes for resolving range overlaid signals in a Doppler weather radar. *Journal of Atmospheric and Oceanic Technology* 16: 1351–1363.

Sakakibara, H., M. Ishihara, A. Tabata, K. Akaeda, and T. Yokoyama. 1991. Evolution and structure of a cold-frontal precipitation system over the subtropical ocean. In *International conference on mesoscale meteorology and TAMEX (preprints)*, Taipei, R. O. C., 173–181. Boston: American Meteorological Society.

Sasaoka, M. 2003. Improvement of wind boundary layer radar using a grouping algorithm. *Tenki, Journal of the Meteorological Society* 50: 161–174 (in Japanese).

Sato, K. 1989. An inertia gravity wave associated with a synoptic-scale pressure trough observed by the MU radar. *Journal of the Meteorological Society of Japan* 67: 325–333.

Sato, K. 1990. Vertical wind disturbances in the troposphere and lower stratosphere observed by the MU radar. *Journal of the Atmospheric Sciences* 47: 2803–2817.

Sato, K. 1993. Small-scale wind disturbances observed by the MU radar during the passage of Typhoon Kelly. *Journal of the Atmospheric Sciences* 50: 519–537.

Sato, T. 1988. Radar principles. In *Lecture notes of International School on Atmospheric Radar (ISAR)*, ed. S. Fukao, 19–53. Kyoto: Kyoto University.

Sato, T., and R.F. Woodman. 1982. Spectral parameter estimation of CAT radar echoes in the presence of fading clutter. *Radio Science* 17: 817–826.

Sato, K., H. Hashiguchi, and S. Fukao. 1995. Gravity waves and turbulence associated with cumulus convection observed with the UHF/VHF clear-air Doppler radars. *Journal of Geophysical Research* 100: 7111–7119.

Sato, K., M. Tsutsumi, T. Sato, A. Saito, Y. Tomikawa, T. Aso, T. Yamauchi, and M. Ejiri. 2006. Program of the Antarctic Syowa MST/IS radar (Pansy). *European Geosciences Union* 8: 1607-796/gra/EGU06-A-05594.

Sato, T., H. Iwai, I. Kimura, S. Fukao, M. Yamamoto, T. Tsuda, and S. Kato. 1990. Computer processing for deriving drop-size distributions and vertical air velocities from VHF Doppler radar spectra. *Radio Science* 25: 961–973.

Sato, T., N. Ao, M. Yamamoto, S. Fukao, T. Tsuda, and S. Kato. 1991. A typhoon observed with the MU Radar. *Monthly Weather Review* 119: 755–768.

Satoh, S., and J. Wurman. 2003. Accuracy of wind fields observed by a bistatic Doppler radar network. *Journal of Atmospheric and Oceanic Technology* 20: 1077–1091.

Sauvageot, H. 1992. *Radar meteorology*, 366 pp. Boston: Artech House.

Schmidt, R.O. 1986. Multiple emitter location and signal parameter estimation. *IEEE Transactions on Antennas and Propagation* AP-34: 276–280.

Sekhon, R.S., and R.C. Srivastava. 1970. Snow-size spectra and radar reflectivity. *Journal of the Atmospheric Sciences* 27: 299–307.

Sekhon, R.S., and R.C. Srivastava. 1971. Doppler radar observations of drop-size distributions in a thunderstorm. *Journal of the Atmospheric Sciences* 28: 983–994.

Seliga, T.A., and V.N. Bringi. 1976. Potential use of radar differential reflectivity measurements at orthogonal polarizations for measuring precipitations. *Journal of Applied Meteorology* 15: 69–76.

Sempre-Torres D., J.M. Porra, and J.D. Creutin. 1994. A general formulation for raindrop size distribution. *Journal of Applied Meteorology* 33: 1494–1502.

Shibagaki, Y., M.D. Yamanaka, H. Hashiguchi, A. Watanabe, H. Uyeda, Y. Maekawa, and S. Fukao. 1997. Hierarchical structures of vertical velocity variations and precipitating clouds near the Baiu frontal cyclone center observed by the MU and meteorological radars. *Journal of the Meteorological Society of Japan* 75: 569–596.

Shibagaki, Y., M.D. Yamanaka, S. Shimizu, H. Uyeda, A. Watanabe, Y. Maekawa, and S. Fukao. 2000. Meso-β to -γ-scale wind circulations associated with precipitating clouds near Baiu front observed by the MU and meteorological radars. *Journal of the Meteorological Society of Japan* 78: 69–91.

Shibagaki, Y., M.D. Yamanaka, M. Kita-Fukase, H. Hashiguchi, Y. Maekawa, and S. Fukao. 2003. Meso-α-scale wind field and precipitating clouds in Typhoon 9426 (Orchid) observed by the MU radar. *Journal of the Meteorological Society of Japan* 81: 211–228.

Shusse, Y., K. Nakagawa, N. Takahashi, S. Satoh, and T. Iguchi. 2009. Characteristics of polarimetric radar variables in three types of rainfalls in a baiu front event over the East China Sea. *Journal of the Meteorological Society of Japan* 87: 865–875.

Siggia, A. 1983. Processing phase codes radar signals with adaptive digital filters. In *21st International conference on radar meteorology (preprints)*, Edmonton, AB, Canada, 167–172. Boston: American Meteorological Society.

Siggia, A.D., and R.E. Passarelli, Jr. 2004. Gaussian model adaptive processor (GMAP) for improved ground clutter cancellation and moment calculation. In *Proceedings. Third European Conference on Radar Meteorology (ERAD)*, Visby, Island of Gotland, Sweden, 67–73.

Silver, S. 1949. *Microwave antenna theory and design*, 623 pp. New York: McGraw-Hill.

Silverman, R.A. 1956. Turbulent mixing theory applied to radio scattering. *Journal of Applied Physics* 27: 690–705.

Skolnik, M.I. ed. 1970. Radar handbook, 1536 pp. New York: McGraw-Hill.

Skolnik, M.I. ed. 1981. *Introduction to radar systems*, 581 pp. 2nd ed. New York: McGraw-Hill.

Skolnik, M.I. ed. 1990. *Radar handbook*, 1200 pp. 2nd ed. New York: McGraw-Hill.

Skolnik, M.I. ed. 2001. *Introduction to radar systems*, 772 pp. 3rd ed. New York: McGraw-Hill.

Smith, P.L. 1984. Equivalent radar reflectivity factor for snow and ice particles. *Journal of Climate and Applied Meteorology* 23: 1258–1260.

Smith, P.L. 1986. On the sensitivity of weather radar. *Journal of Atmospheric and Oceanic Technology* 3: 704–713.

Smith, S.A., D.C. Fritts, and T.E. VanZandt. 1987. Evidence of a saturation spectrum of atmospheric waves. *Journal of the Atmospheric Sciences* 44: 1404–1410.

Spano, E., and O. Ghebrebrhan. 1996a. Pulse coding techniques for ST/MST radar systems: A general approach based on a matrix formulation. *IEEE Transactions on Geoscience and Remote Sensing* GE-34: 304–316.

Spano, E., and O. Ghebrebrhan. 1996b. Sequences of complementary codes for the optimum decoding of truncated ranges and high sidelobe suppression factors for ST/MST radar systems. *IEEE Transactions on Geoscience and Remote Sensing* GE-34: 330–345.

Srivastava, R.C. 1967. On the role of coalescene between raindrops in shaping their size distribution. *Journal of the Atmospheric Sciences* 24: 287–292.

Srivastava, R.C. 1971. Size distribution of raindrops generated by their breakup and coalescence. *Journal of the Atmospheric Sciences* 28: 410–415.

Srivastava, R.C., A. R. Jameson, and P. H. Hildebrand. 1979. Time-domain computation of mean and variance of Doppler spectra. *Journal of Applied Meteorology* 18: 189–194.

Straka, J.M., D. Zrnić, A.V. Ryzhkov. 2000. Bulk hydrometeor classification and quantification using polarimetric radar data: Synthesis of relations. *Journal of Applied Meteorology* 39: 1341–1372.

Stratton, J.A. 2007. *Electromagnetic theory*, 615 pp. Piscataway: IEEE Press.

Stutzman, W.L. 1998. Estimating directivity and gain of antennas. *IEEE Antennas and Propagation Magazine* 40: 7–11.

Sumi, A. 1989. Short-period fluctuation of the lower tropospheric winds observed by the MU radar. *Journal of the Meteorological Society of Japan* 67: 167–175.

Tabata, A., H. Sakakibara, M. Ishihara, K. Matsuura, and Z. Yanagisawa. 1992. A general view of the structure of Typhoon 8514 observed by dual-Doppler radar—From outer rainbands to eyewall clouds. *Journal of the Meteorological Society of Japan* 70: 897–917.

Takeda, S., T. Nakamura, and T. Tsuda. 2001. An improvement of wind velocity estimation from radar Doppler spectra in the upper mesosphere. *Annales Geophysicae* 19: 837–843.

Tatarskii, V.I. 1971. *The effects of the turbulent atmosphere on wave propagation*, 472 pp. Translated from Russian, Jerusalem.

Teschl, T., W.L. Randeu, M. Schönhuber, and R. Teschl. 2008. Simulation of polarimetric radar variables in rain at S-, C- and X-band wavelengths. *Advances in Geosciences* 16: 27–32

Teshiba, M., H. Hashiguchi, S. Fukao, and Y. Shibagaki. 2001. Typhoon 9707 observations with the MU radar and L-band boundary layer radar. *Annales Geophysicae* 19: 925–931.

Teshiba, M., H. Fujita, H. Hashiguchi, Y. Shibagaki, M.D. Yamanaka, and S. Fukao. 2005. Detailed structure within a tropical cyclone "eye." *Geophysical Research Letters* 32: L24805. doi:10.1029/2005GL023242.

Testud, J. 1982. Three-dimensional wind field analysis from Doppler radar data. In *Mesoscale meteorology—theories, observations and models*, eds. D.L. Lilly, and T. Gal-Chen, 711–754. Dordrecht: D. Reidel Publishing.

Torlaschi, E., and A.R. Holt. 1993. Separation of propagation and backscattering effects in rain for circular polarization diversity S-band radar. *Journal of Atmospheric and Oceanic Technology* 10: 465–477.

Townsend, A.A. 1965. Excitation of internal waves by a turbulent boundary layer. *Journal of Fluid Mechanics* 22: 241–252.

Townsend, A.A. 1966. Internal waves produced by a convective layer. *Journal of Fluid Mechanics* 24: 307–319.

Tsuda, T. 2001. Measurements of atmospheric temperature with the RASS. *Choonpa Techno* 13: 18–22 (in Japanese).

Tsuda, T., T. Sato, K. Hirose, S. Fukao, and S. Kato. 1986. MU radar observations of the aspect sensitivity of backscattered VHF echo power in the troposphere and lower stratosphere. *Radio Science* 21: 971–980.

Tsuda, T., Y. Masuda, H. Inuki, K. Takahashi, T. Takami, T. Sato, S. Fukao, and S. Kato. 1989a. High time resolution monitoring of tropospheric temperature with a Radio Acoustic Sounding System (RASS). *Pure and Applied Geophysics* 130: 497–507.

Tsuda, T., T. Inoue, D.C. Fritts, T.E. VanZandt, S. Kato, T. Sato, and S. Fukao. 1989b. MST radar observations of a saturated gravity wave spectrum. *Journal of the Atmospheric Sciences* 46: 2440–2447.

Tsuda, T., S. Kato, T. Yokoi, T. Inoue, M. Yamamoto, T.E. VanZandt, S. Fukao, and T. Sato. 1990a. Gravity waves in the mesosphere observed with the middle and upper atmosphere radar. *Radio Science* 26: 1005–1018.

Tsuda, T., Y. Murayama, M. Yamamoto, S. Kato, and S. Fukao. 1990b. Seasonal variation of momentum flux in the mesosphere observed with the MU radar. *Geophysical Research Letters* 17: 725–728.

Tsuda, T., T. Adachi, Y. Masuda, S. Fukao, and S. Kato. 1994. Observations of tropospheric temperature fluctuations with the MU radar-RASS. *Journal of Atmospheric and Oceanic Technology* 11: 50–62.

Tsuda, T., T.E. VanZandt, and H. Saito. 1997. Zenith-angle dependence of VHF specular reflection echoes in the lower atmosphere. *Journal of Atmospheric and Terrestrial Physics* 59: 766–776.

Tsuda, T., M. Miyamoto, and J. Furumoto. 2001. Estimation of a humidity profile using turbulence echo characteristics. *Journal of Atmospheric and Oceanic Technology* 18: 1214–1222.

Tsutsumi, M., T. Tsuda, and T. Nakamura. 1994. Temperature fluctuations near the mesopause inferred from meteor observations with the middle and upper atmosphere radar. *Radio Science* 29: 599–610.

Ulaby, F.T., R.K. Moore, and A.K. Fung. 1981. *Microwave remote sensing I, microwave remote sensing fundamentals and radiometry*, 456 pp. Norwood: Artech House.

Ulaby, F.T., R.K. Moore, and A.K. Fung. 1986. *Microwave remote sensing III, from theory to application*, 2162 pp. Norwood: Artech House.

Ulbrich, C.W. 1983. Natural variations in the analytical form of the raindrop-size distribution. *Journal of Climate and Applied Meteorology* 22: 1764–1775.

Umemoto, Y., M. Teshiba, Y. Shibagaki, H. Hashiguchi, M.D. Yamanaka, S. Fukao, and X-BAIU-99 and X-BAIU-02 Observational Groups. 2004. Combined wind profiler-weather radar observations of orographic rainband around Kyushu, Japan in the Baiu season. *Annales Geophysicae* 22: 3971–3982.

Ushiyama, T., M. Kawashima, and Y. Fujiyoshi. 2003. Heating distribution by cloud systems derived from Doppler radar observation in TOGA-COARE. *Journal of the Meteorological Society of Japan* 81: 1407–1434.

Ushiyama, T., M. Katsumata, and R. Shiooka. 2005. Idealized simulation of dual Doppler radar observation using numerically simulated clouds. *JAMSTEC Report of Research and Development* 1: 37–43.

Uyeda, H., and D.S. Zrnić. 1986. Automatic detection of gust fronts. *Journal of Atmospheric and Oceanic Technology* 3: 36–50.

Van Baelen, J.S., A.D. Richmond, T. Tsuda, S.K. Avery, S. Kato, S. Fukao, and M. Yamamoto. 1991. Radar interferometry technique and anisotropy of the echo power distribution: First results. *Radio Science* 26: 1315–1326.

Van de Hulst, H.D. 1957. *Light scattering by small particles*, 470 pp. New York: Wiley.

Van Vleck, J.H. 1947a. Absorption of microwaves by oxygen. *Physical Review* 71: 413–424.

Van Vleck, J.H. 1947b. The absorption of microwaves by uncondensed water vapor. *Physical Review* 71: 425–433.

VanZandt, T.E., and R.A. Vincent. 1983. Is VHF Fresnel reflectivity due to low-frequency waves. In *Handbook for MAP*, vol. 9, 78–80. Urbana: ICSU Scientific Committee on Solar-Terrestrial Physics (SCOSTEP).

Vincent, R.A., and I.M. Reid. 1983. HF Doppler measurements of mesospheric gravity wave momentum fluxes. *Journal of the Atmospheric Sciences* 40: 1321–1333.

Vincent, R.A., S. Dullaway, A. MacKinnon, I.M. Reid, F. Zink, P.T. May, and B.H. Johnson. 1998. A VHF boundary layer radar: first results. *Radio Science* 33: 845–860.

Vivekanandan, J., G. Zhang, and E. Brandes. 2004. Polarimetric radar estimators based on a constrained gamma drop size distribution model. *Journal of Applied Meteorology* 43: 217–230.

Wada, M., and H. Uyeda. 2011. Solid-state weather radar which reached the practical use stage. In *35th Conference on radar meteorology (preprints)*. Pittsburgh: American Meteorological Society, p12.163.

Wait, J.R. 1962. *Electromagnetic waves in stratified media*, 372 pp. Oxford: Pergamon.

Wakasugi, K., A. Mizutani, M. Matsuo, S. Fukao, and S. Kato. 1986. A direct method for deriving drop-size distribution and vertical air velocities from VHF Doppler radar spectra. *Journal of Atmospheric and Oceanic Technology* 3: 623–629.

Wakimoto, R.M. 1985. Forecasting dry microburst activity over the high plains. *Monthly Weather Review* 113: 1131–1143.

Waldteufel, P., and H. Corbin. 1979. On the analysis of single Doppler data. *Journal of Applied Meteorology* 18: 532–542.

Wang, Y., V. Chandrasekar, and B. Dolan. 2008. Development of scan strategy for dual Doppler retrieval in a networked radar system. In *IEEE international of geoscience and remote sensing symposium, 2008*, vol. 5, V-322–V-325.

Watanabe, A., S. Fukao, M.D. Yamanaka, A. Sumi, and H. Uyeda. 1994. A rotor circulation near the Baiu front observed by the MU radar. *Journal of the Meteorological Society of Japan* 72: 91–105.

Weinman, J.A., R. Meneghini, and K. Nakamura. 1990. Retrieval of precipitation profiles from airborne radar and passive radiometer measurements: Comparison with dual-frequency radar measurements. *Journal of Applied Meteorology* 29: 981–993.

Weinstock, J. 1978. Vertical turbulent diffusion in a stably stratified fluid. *Journal of the Atmospheric Sciences* 35: 1022–1027.

Weinstock, J. 1981. Energy dissipation rates of turbulence in the stable free atmosphere. *Journal of the Atmospheric Sciences* 38: 880–883.

Wexler, R. and D. Atlas. 1963. Radar reflectivity and attenuation of rain. *Journal of Applied Meteorology* 2: 276–280.

Wilczak, J.M., R.G. Strauch, F.M. Ralph, B.L. Weber, D.A. Merritt, J.R. Jordan, D.E. Wolfe, L.K. Lewis, D.B. Wuertz, J.E. Gaynor, S.A. McLaughlin, R.R. Rogers, A.C. Riddle, and T.S. Dye. 1995. Contamination of wind profiler data by migrating birds: Characteristics of corrupted data and potential solutions. *Journal of Atmospheric and Oceanic Technology* 12: 449–467.

Williams, C.R., W.L. Ecklund, and K.S. Gage. 1995. Classification of precipitating clouds in the tropics using 915-MHz wind profilers. *Journal of Atmospheric and Oceanic Technology* 12: 996–1012.

Willis, P.T. 1984. Functional fits to some observed drop size distributions and parameterization of rain. *Journal of the Atmospheric Sciences* 41: 1648–1661.

Wilson, R. 2004. Turbulent diffusivity in the free atmosphere inferred from MST radar measurements: A review. *Annales Geophysicae* 22, 3869–3887.

Wolfson, M. M. 1983. Doppler radar observations of an Oklahoma downburst. In *21st Conference on radar meteorology (preprints)*, 590–595. Edmonton: American Meteorological Society.

Wood, V.T., and R.A. Brown. 1983. Single Doppler velocity signatures: An atlas of patterns in clear air/widespread precipitation and convective storms. In *NOAA technical memorandum ERL NSSL-95*, 71 pp. Norman: NOAA Environmental Research Laboratories.

Woodman R.F. 1980. High altitude-resolution stratospheric measurements with the Arecibo 2380-MHz radar. *Radio Science* 15: 423–430.

Woodman, R.F., and A. Guillén. 1974. Radar observations of winds and turbulence in the stratosphere and mesosphere. *Journal of the Atmospheric Sciences* 31: 493–505.

Worthington, R.M., R.D. Palmer, and S. Fukao. 1999. Complete maps of the aspect sensitivity of VHF atmospheric radar echoes. *Annales Geophysicae* 17: 1116–1119.

Wurman, J., S. Heckman, and D. Boccipio. 1993. A bistatic multiple-Doppler radar network. *Journal of Applied Meteorology* 32: 1802–1814.

Wurman, J., J. Straka, and E. Rasmussen. 1996. Fine scale Doppler radar observation of tornadoes. *Science* 272: 1774–1777.

Yamada, Y. 1997. Numerical estimation of error variance in horizontal divergence for the adjustment of vertical winds derived from conical-scan-based dual-Doppler radar data based on the "floating boundary condition" concept. *Papers in Meteorology and Geophysics* 48: 49–65.

Yamamoto, M., T. Tsuda, S. Kato, T. Sato, and S. Fukao. 1987. A saturated inertia gravity wave in the mesosphere observed by the middle and upper atmosphere radar. *Journal of Geophysical Research* 92: 11993–11999.

Yamamoto, M., T. Tsuda, S. Kato, T. Sato, and S. Fukao, 1988. Interpretation of the structure of mesospheric turbulence layers in terms of inertia gravity waves. *Physica Scripta* 37: 645–650.

Yamamoto, M., S. Fukao, R.F. Woodman, T. Ogawa, T. Tsuda, and S. Kato. 1991. Mid-latitude E-region field-aligned irregularities observed with the MU radar. *Journal of Geophysical Research* 96: 15943–15949.

Yamamoto, M.K., H. Hashiguchi, S. Fukao, Y. Shibano, and K. Imai. 2002. Development of a transportable 3-GHz wind profiler for wind and precipitation studies. *Journal of the Meteorological Society of Japan* 80: 273–283.

Yamamoto, M.K., M. Oyamatsu, T. Horinouchi, H. Hashiguchi, and S. Fukao. 2003a. High time resolution determination of the tropical tropopause by the equatorial atmosphere radar. *Geophysical Research Letters* 30: 2094. doi:10.1029/2003GL018072.

Yamamoto, M.K., M. Fujiwara, T. Horinouchi, H. Hashiguchi, and S. Fukao. 2003b. Kelvin-Helmholtz instability around the tropical tropopause observed with the equatorial atmosphere radar. *Geophysical Research Letters* 30: 1476. doi:10.1029/2002GL016685.

Yamanaka, M.D., S. Fukao, H. Matsumoto, T. Sato, T. Tsuda, and S. Kato. 1989. Internal gravity wave selection in the upper troposphere and lower stratosphere observed by the MU radar: Preliminary results. *Pure and Applied Geophysics* 130: 481–495.

Yamauchi, H., O. Suzuki, and K. Akaeda. 2006. A hybrid multi-PRI method to dealias Doppler velocities. *Scientific Online Letters on the Atmosphere* 2: 92–95.

Yamauchi, H., O. Suzuki, and K. Akaeda. 2007. Range extension of Doppler radar by combined use of low-PRF and phase diversity processed dual-PRF observations. In *33rd Conference on radar meteorology (preprints)*. Cairns: American Meteorological Society, p7.5.

Yeh, K.C., and C.H. Liu. 1972. *Theory of ionospheric waves*, 464 pp. New York: Academic.

Yoshizaki, M., and H. Seko. 1994. A retrieval of thermodynamic and microphysical variables by using wind data in simulated multi-cellular convective storms. *Journal of the Meteorological Society of Japan* 72: 31–42.

Yu, T.-Y., and R.D. Palmer. 2001. Atmospheric radar imaging using multiple-receiver and multiple-frequency techniques. *Radio Science* 36: 1493–1503. doi:10.1029/2000RS002622.

Yu, T.-Y., and W.O.J. Brown. 2004. High-resolution atmospheric profiling using combinated spaced antenna and range imaging techniques. *Radio Science* 39: 1011. doi:10.1029/2003RS002907.

Yu, T.-Y., J. Furumoto, and M. Yamamoto. 2010. Clutter suppression for high-resolution atmospheric observations using multiple receivers and multiple frequencies. *Radio Science* 45: RS4011. doi:10.1029/2009RS004330.

Zhang, P., S. Liu, and Q. Xu. 2005. Identifying Doppler velocity contamination caused by mitigating birds, Part I: Feature extraction and quantification. *Journal of Atmospheric and Oceanic Technology* 22: 1105–1113.

Zhong, S., J.D. Fast, and X. Bian. 1996. A case study of the Great Plains low-level jet using wind profiler network data and a high-resolution mesoscale model. *Monthly Weather Review* 124: 785–806.

Ziemer, R.E., W.H. Tranter, and D.R. Fannin. 1998. *Signals and systems: Continuous and discrete*. 4th ed, 622 pp. New Jersey: Prentice Hall.

Zrnić, D.S. 1979. Estimation of spectral moments for weather echoes. *IEEE Transactions on Geoscience Electronics* GE-17: 113–128.

Zrnić, D.S., and P. Mahapatra. 1985. Two methods of ambiguity resolution in pulsed Doppler weather radars. *IEEE Transactions on Aerospace and Electronic Systems* 21: 470–483.

Zrnić, D.S., A. Ryzhkov, J. Straka, Y. Liu, and J. Vivekanandan. 2001. Testing a procedure for automatic classification of hydrometeor types. *Journal of Atmospheric and Oceanic Technology* 18: 892–913.

Zrnić, D.S., V.M. Melnikov, and J.K. Carter. 2006. Calibrating differential reflectivity on the WSR-88D. *Journal of Atmospheric and Oceanic Technology* 23: 892–913.

Zrnić, D.S., V.M. Melnikov, and R.J. Doviak. 2012. A draft report on issues and challenges for polarimetric measurement of weather with an agile-beam phased array radar. http://publications.nssl.noaa.gov/mpar_reports/MPAR-WEB_RPT.pdf,132pp.

Index

S. Fukao and K. Hamazu, *Radar for Meteorological and Atmospheric Observations*,
DOI 10.1007/978-4-431-54334-3, © Springer Japan 2014